

C. Bröcker · A. Matzenmiller

An enhanced concept of rheological models to represent nonlinear thermoviscoplasticity and its energy storage behavior

Received: 29 May 2012 / Accepted: 13 August 2012 / Published online: 2 November 2012
© Springer-Verlag 2012

Abstract An enhanced rheological network is presented for the material modeling of thermoviscoplasticity. By introducing new basic elements, nonlinear isotropic and kinematic hardening may be depicted as well as an improved description of energy storage and dissipation during plastic deformations. Satisfying the thermomechanical consistency, the yield function and the flow rule are directly deduced from the stress equilibrium and the kinematics of the rheological network by means of simple algebraic calculations. Novel approaches are proposed to account for a process-dependent energy storage also for the case of ideal plasticity. The resulting energy storage behavior is investigated and validated by means of the simulation of tension test data.

Keywords Rheological models · Thermoviscoplasticity · Novel ideal bodies · Representation of energy storage/dissipation

Mathematics Subject Classification (2010) Primary classification 74A20 · Secondary classification 74C10 · 74A15 · 74F05

1 Introduction

Material modeling by means of rheological networks offers a very simple and straight forward approach for the characterization and description of complex material behavior. Within the concept of rheological models, basic bodies are defined for particular aspects of the real constitutive behavior, like the Hooke body (ideal elastic), the St.-VENANT element (ideal plastic) or the NEWTON fluid (ideal viscous), which are represented visually by simple icons like the spring, the friction element (block with dry friction) or the dashpot [31]. By assembling networks of the basic elements in series or in parallel arrangement, more complicated ideal bodies may be generated, for which the complex constitutive equations arise from the elementary material relations of the single bodies by means of simple algebraic calculations. Rheological models provide a physically plausible constitutive approach, which is detached from the actual processes and activities acting on the microscopic level of the material. However, the real material behavior may be approximated reliably, if the free material parameters are adjusted well to the experimental test data.

In the book of Reiner [31], one of the pioneers in rheological modeling, the basic elements, mentioned afore, are given and various models of viscoelasticity and viscoplasticity are assembled. Krawietz [19] specifies a new element for the description of plastic behavior without an elastic range (endochronic plasticity—see [40]). This element is also applied for the modeling of nonlinear kinematic hardening with saturation. Additionally, in Krawietz [19], a separate rheological body is introduced to represent thermal strains. Both of these elements are applied in the work of Lion [22,24] for constructing a viscoplastic model without a yield surface

Communicated by Andreas Öchsner.

C. Bröcker · A. Matzenmiller (✉)
Institute of Mechanics (Mechanical Engineering), University of Kassel, Mönchebergstr. 7, 34125 Kassel, Germany
E-mail: amat@uni-kassel.de

for the constitutive representation of filled rubber as well as for a second strain rate-dependent model of metal plasticity with a yield surface in [23,25]. The rheological model of Lion [23] is adopted, for example, in [34] in the context of plastic forming under consideration of thermal effects. Also, in [18,32], the material modeling is based on rheological networks with endochronic elements for the description of thermoplastic sealings and fiber glass reinforced thermoplastics. Moreover, in [33], even distortional hardening is represented by means of two-dimensional rheological networks. In numerous other publications of material theory, rheological models are taken into account, see e.g., [1,9–11,26,36,41,42]. The procedure of material modeling by means of rheological networks is common especially in the field of viscoelasticity, for example, in the case of the three parameter model of the standard linear solid or the generalized MAXWELL or KELVIN bodies—see also [8,39]. However, in the framework of plasticity, the rheological networks are often used as a motivation or as the underlying structure of the final material model—see [9,10], but the constitutive equations are not deduced from the rheological network itself as it is usually done for models of viscoelasticity.

In the context of thermomechanical modeling for metals, the appropriate function for the free energy and especially for its plastic part is difficult to establish such that a physically reasonable material theory reproduces the hardening behavior as well as the energy storage and the dissipation during plastic deformations as measured in the experiment. Different models for the plastic part of the free energy, proposed in [5,6,12–15,17], already allow for a better representation of the energy transformation. In a recent work, Shutov and Ihlemann [34] propose a novel approach to improve the energy storage and dissipation behavior in metal plasticity based on an additional fraction of the free energy function—denoted as “detached energy,” which is detached from the storage process of energy due to the hardening of the material model. However, the key questions are still open: Which structure should the free energy have, on which internal variables should the free energy depend on and how do they evolve during a given mechanical process? The answer thereon is quite simple from the point of view of rheological models: The free energy of the material model follows directly and necessarily from the energy, stored in all elements, introduced into the network. However, until now, there is for instance no basic element for representing isotropic hardening. Usually, this type of hardening is only accounted for in the rheological model by means of a process-dependent yield stress in the friction element, which does not contribute to the free energy. Such an approach might be completely sufficient, as far as only mechanical aspects of the material model are of interest. Otherwise, a contribution of isotropic hardening may only be postulated physically plausible to the free energy according to the present state of the art.

In the paper at hand, the procedure of material modeling by means of rheological networks is enhanced, allowing for a better representation of complex thermoviscoplasticity. A new element is introduced for the description of isotropic hardening, and some already known basic elements are modified or specified more precisely. Moreover, the proposed model is focused also on the representation of energy storage and dissipation during plastic flow of metals. Based on the work of Helm [13,14] and Chaboche [5], where also ideal plasticity is related to energy storage, it is assumed that plastic work in the friction element is gathered completely as free energy in order to improve the description of energy transformation. However, in order to avoid an overestimation of energy storage through this assumption, the friction element is put in series with a novel dissipative strain element, which limits the resulting strain and, therefore, the work spent on the friction body. Evaluating the second law of thermodynamics, the constitutive relations of the thermoviscoplastic model are directly deduced from the definitions of the basic elements as well as the decompositions of stress and strain, which hold true for the rheological network. By this way of proceeding, the thermomechanical consistency of the enhanced model can be easily proven and, moreover, the well-known yield function and the flow rule result most naturally.

In order to clarify the main ideas of the paper, the modeling approaches are restricted for one spatial dimension only. A generalization of the proposed concept of enhanced rheological modeling for small deformations representing three-dimensional tensor valued quantities turns out in a completely analogous procedure as in the uniaxial case, which will be published in a forthcoming paper. Moreover, also the extension of the model for large deformations seems to be straight forward, for example, according to the procedure in [23].

In the second chapter of the paper, the mechanical dissipation and the equation of heat conduction are provided in a general form. In Sect. 3, the known ideal bodies are introduced and new, respectively, modified ones are defined. An enhanced rheological model of thermoviscoplasticity is assembled in Sect. 4 and its constitutive equations are deduced. In the following chapter, the material model is validated with regard to the energy transformation during plastic flow. Section 6 presents some studies concerning the energy storage behavior. In the last chapter, further approaches, accounting for a process-dependent energy storage for ideal plasticity, are proposed and validated on the basis of simulations and test data.

2 Dissipation, equation of heat conduction and energy transformation

2.1 Mechanical dissipation

The internal dissipation δ follows from the balance equations for energy and entropy in combination with the second law of thermodynamics—see [10]:

$$\delta = -\dot{\psi} + \frac{1}{\rho} \sigma \dot{\varepsilon} - \dot{\theta} s - \frac{1}{\rho \theta} q g \geq 0, \quad (1)$$

where ψ is the free energy (Helmholtz free energy). Furthermore, ρ is the mass density, σ the stress, θ the temperature, s the entropy, q the heat flux and $g = \partial\theta/\partial x$ the temperature gradient. An additive decomposition of the strain¹ is assumed according to

$$\varepsilon = \varepsilon_{\text{el}} + \varepsilon_{\text{i}} + \varepsilon_{\text{th}} \quad (2)$$

into a purely elastic part ε_{el} , a purely inelastic one ε_{i} as well as a purely thermal contribution ε_{th} , which shall evolve proportionally to the temperature change

$$\dot{\varepsilon}_{\text{th}} = \alpha \dot{\theta} \quad (3)$$

with α as the thermal expansion coefficient. The free energy ψ may be initially arranged in general form as a function of the elastic strain ε_{el} , the temperature θ , the temperature gradient² g , as well as further internal variables a_1, \dots, a_n of the strain type, such as inelastic “back strains” of kinematic hardening or other internal (hardening) variables, for example, dislocation densities, phase transition values and others:

$$\psi = \psi(\varepsilon_{\text{el}}, \theta, g, a_1, \dots, a_n) = \psi_{\text{te}}(\varepsilon_{\text{el}}, \theta, g) + \psi_{\text{i}}(\theta, g, a_1, \dots, a_n). \quad (4)$$

Note that the free energy may be also split into a thermoelastic and an inelastic part ψ_{te} and ψ_{i} as often assumed in the literature. Using the time derivative of the free energy (4) and the strain decomposition (2) with (3), the dissipation inequality (1) can be rearranged as

$$\delta = \left(\frac{1}{\rho} \sigma - \frac{\partial \psi}{\partial \varepsilon_{\text{el}}} \right) \dot{\varepsilon}_{\text{el}} - \left(\frac{\partial \psi}{\partial \theta} - \frac{1}{\rho} \sigma \alpha + s \right) \dot{\theta} - \frac{\partial \psi}{\partial g} \dot{g} + \frac{1}{\rho} \sigma \dot{\varepsilon}_{\text{i}} - \sum_{j=1}^n \frac{\partial \psi}{\partial a_j} \dot{a}_j - \frac{1}{\rho \theta} q g \geq 0. \quad (5)$$

To satisfy the condition of $\delta \geq 0$ for all possible thermomechanical processes, the prefactors in front of the time derivatives of the elastic strain, the temperature and the temperature gradient $\dot{\varepsilon}_{\text{el}}$, $\dot{\theta}$ and \dot{g} have to vanish. Hence, potential relations result for the stress and the entropy according to

$$\sigma = \rho \frac{\partial \psi}{\partial \varepsilon_{\text{el}}} \quad (6)$$

and

$$s = \frac{1}{\rho} \sigma \alpha - \frac{\partial \psi}{\partial \theta} = \alpha \frac{\partial \psi}{\partial \varepsilon_{\text{el}}} - \frac{\partial \psi}{\partial \theta} \quad (7)$$

as well as the term

$$\frac{\partial \psi}{\partial g} = 0. \quad (8)$$

Equation (8) states that the free energy (4) has to be independent of the temperature gradient g :

$$\psi = \psi(\varepsilon_{\text{el}}, \theta, a_1, \dots, a_n) = \psi_{\text{te}}(\varepsilon_{\text{el}}, \theta) + \psi_{\text{i}}(\theta, a_1, \dots, a_n). \quad (9)$$

¹ In the literature, the strain is usually separated into an elastic and an inelastic part, only. The strain decomposition (2) has already been used, for example, by Lion and Sedlan [23,25]. In Appendix A.6, a comparison is shown between the representations of thermoelasticity associated with both alternative approaches of strain decompositions.

² Since the heat flux q has to be a function of the temperature gradient g , this variable is usually added to the list of arguments of the free energy—see e.g., [10].

Moreover, the remaining three summands of the internal dissipation (5) may be split up according to

$$\delta = \delta_{\text{th}} + \delta_{\text{M}} \geq 0 \quad (10)$$

into the thermal δ_{th} and the mechanical contribution δ_{M} , which both have to be nonnegative in any case. The condition for the thermal dissipation³

$$\delta_{\text{th}} := -\frac{1}{\rho\theta} q g \geq 0 \quad (11)$$

is satisfied by assuming that the heat flux q is proportional to the negative temperature gradient $-g$, leading directly to FOURIER'S model of heat conduction

$$q = -k g, \quad (12)$$

where k is the thermal conductivity of the material. Therefore, only the inequality for the mechanical dissipation

$$\delta_{\text{M}} := \underbrace{\frac{1}{\rho} \sigma \dot{\varepsilon}_i}_{p_{\text{p}}} - \underbrace{\sum_{j=1}^n \frac{\partial \psi}{\partial a_j} \dot{a}_j}_{p_{\text{s}}} \geq 0 \quad (13)$$

is left from the expression for the internal dissipation in (5). The first term p_{p} in (13) comprises the total inelastic stress power. The second term p_{s} encloses the entire power of all conjugated internal forces $A_j = \rho \partial \psi / \partial a_j$ at the internal strain rates \dot{a}_j , stored in the material. In the case of thermoplasticity of metals, this power is required to change the materials microstructure during plastic flow, for example, due to the formation of new dislocations, the motion of dislocations along grain boundaries or the blocking of slip planes at obstacles and so on. These processes induce local internal stress fields, causing macroscopic hardening of the material. Hence, not the entire (plastic) stress power p_{p} is dissipated and converted into heat, but the power p_{s} is stored in the material. Thus, only the difference

$$p_{\text{d}} := p_{\text{p}} - p_{\text{s}} = \delta_{\text{M}} \quad (14)$$

contributes to the dissipative heating of the inelastic material. The energy, stored in the material during plastic deformation, is also called “stored energy of cold work” [3]. First investigations into this matter have been made by Taylor and Quinney [37].

2.2 Equation of heat conduction

The equation of heat conduction is deduced from the local energy balance—see [10]:

$$\dot{e} = \frac{1}{\rho} \sigma \dot{\varepsilon} - \frac{1}{\rho} \operatorname{div} q + b. \quad (15)$$

Besides the above mentioned variables, here e specifies the internal energy and b is an internal volumetric heat source. The free energy ψ can be related to the internal energy e by means of the LEGENDRE transformation with respect to entropy s and temperature θ according to

$$\psi = e - \theta s. \quad (16)$$

The local energy balance (15) is transferred with FOURIER'S model of heat conduction (12) and the derivatives of the free energy (16) and (9) with respect to time as well as with the potential relations for the stress (6) and the entropy (7) into the form

$$\theta \dot{s} = \frac{1}{\rho} k \operatorname{div}(g) + b + \delta_{\text{M}}. \quad (17)$$

³ The symbol “:=” in (11) represents the defining equal sign.

By means of the time derivative of the entropy (7) for the general approach of the free energy (9), and the definition of the heat capacity at constant deformation—see [10]—according to

$$c_{\text{def}} := \theta \frac{\partial s(\varepsilon_{\text{el}}, \theta, a_1, \dots, a_n)}{\partial \theta}, \quad (18)$$

the equation of heat conduction is obtained from (17) in a general, material independent formulation⁴:

$$c_{\text{def}} \dot{\theta} = \underbrace{-\theta \frac{\partial s}{\partial \varepsilon_{\text{el}}} \dot{\varepsilon}_{\text{el}}}_{-p_e} + \underbrace{\frac{1}{\rho} k \operatorname{div}(g) + b}_{p_Q} + \underbrace{\delta_M}_{p_d} - \underbrace{\theta \sum_{j=1}^n \frac{\partial s}{\partial a_j} \dot{a}_j}_{-p_i}. \quad (19)$$

The thermoelastic coupling term p_e , also called piezocaloric coupling term, represents a power in the elastic strain rate $\dot{\varepsilon}_{\text{el}}$, which, however, is not related to the elastic stress power $1/\rho \sigma \dot{\varepsilon}_{\text{el}}$. Instead, p_e causes cooling of the body due to expansion and heating in the case of compression of the material. The first summand in p_Q describes the heat conduction process in the body at hand, whereas the second summand includes the specific volumetric heat source b in the material, as they may occur, for example, due to inductive heating or radioactive decay. The last term p_i describes a thermoinelastic coupling, which stands in analogy to its thermoelastic counterpart p_e and provides a positive or negative heat contribution depending on the evolution of the internal strains a_j . Recall, the dissipative power term p_d , given in (14), has been already discussed.

2.3 Energy transformation behavior of metals

In order to quantify roughly the dissipative nature of metals during plastic flow, the energy transformation ratio φ is often used and defined as the quotient

$$\varphi := \frac{\psi_i}{w_p} \quad (20)$$

of the plastic stored energy ψ_i —cf. (9)—divided by the entire plastic work

$$w_p = \int_0^t p_p(\tau) d\tau \quad (21)$$

—see [6, 7]. This energy ratio shows its maximum at the beginning of plastic loading and reduces afterwards—see [7, 13, 28, 29].

In commercial FE-tools like LS-DYNA⁵ or ABAQUS⁶ as well as often in scientific publications, for example, in [35], the dissipation power p_d in the equation of heat conduction is assessed as a part of the plastic stress power p_p by introducing the TAYLOR-QUINNEY coefficient γ [37]:

$$p_d := \gamma p_p = \gamma \frac{1}{\rho} \sigma \dot{\varepsilon}_p. \quad (22)$$

Here, the multiplier γ is a constant factor less than one. Typically, values of $\gamma = 0.85, \dots, 0.95$ are selected for steel sorts—see also [35], resulting with regard to (20) in a constant energy transformation ratio

$$\varphi = 1 - \gamma \quad (23)$$

throughout the entire process of plastic flow, which, however, clearly contradicts recent experimental observations [7, 13, 28, 29]. Depending on the current state of plastic deformation of a special process and the value chosen for the TAYLOR-QUINNEY coefficient γ , the dissipation power p_d is obviously either over- or underestimated.

⁴ Generally, the heat capacity c_{def} in (19) depends particularly on the temperature θ as well as on other internal variables according to (18) and, in special cases, may be assumed approximately as constant in the course of linearization.

⁵ Hallquist, J.O.: LS-DYNA Theory Manual, Version November 2005. Livermore Software Technology Corporation (LSTC), Livermore, California (2005).

⁶ Abaqus Theory Manual, Version 6.7. Simulia, Providence, Rhode Island, USA (2007).

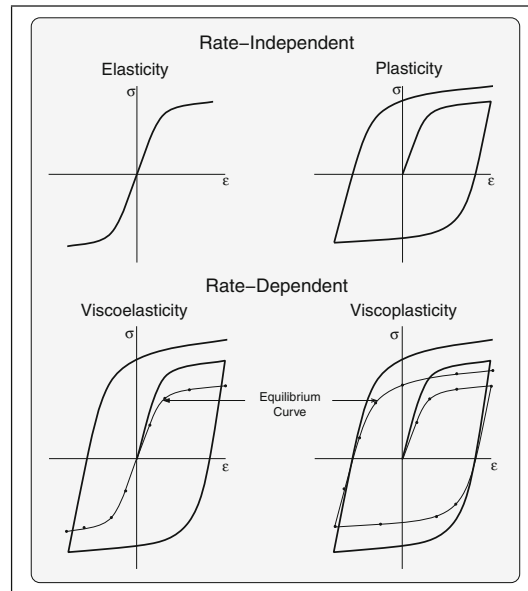


Fig. 1 Overview of different behavior of materials and model types according to Haupt [10]

3 Material modeling based on rheological networks

Figure 1 gives an overview of the most common classes of material models for solids⁷ and their characteristic stress-strain diagrams according to Haupt [10]. While the elasticity and viscoelasticity models are applied mostly in the context of elastomeric or duromeric plastics, the inelastic material models of plasticity and viscoplasticity are used especially to describe the mechanical behavior of metals subjected to large irreversible deformations. The viscoelastic and viscoplastic models show different stress-strain behavior for varying loading rates, whereas the stress response in the case of elasticity or plasticity theory is always identical for any loading rate.

Preliminary remarks

The “arclength” \bar{a} of a variable a is a functional and may be defined as the time integral of the time rate of its absolute value according to

$$\bar{a} := \int_0^t |\dot{a}(\tau)| d\tau = \int_0^t \dot{\bar{a}}(\tau) d\tau \quad (24)$$

with

$$\dot{\bar{a}} := |\dot{a}|. \quad (25)$$

The variable $a = |a| \operatorname{sgn}(a)$ can be split into its absolute value and its algebraic sign⁸. Hence, using (25), the rate \dot{a} can be decomposed into the product

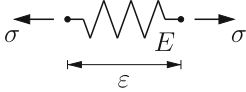
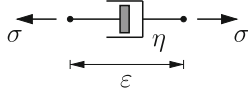
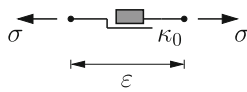
$$\dot{a} = |\dot{a}| \operatorname{sgn}(\dot{a}) = \dot{\bar{a}} \operatorname{sgn}(\dot{a}), \quad (26)$$

where the algebraic sign $\operatorname{sgn}(\dot{a})$ can be interpreted as the “direction of evolution” of the rate \dot{a} , that is, $\operatorname{sgn}(\dot{a})$ indicates whether a growth or decrease in a occurs.

⁷ Figure 2 shows simple possibilities to realize these types of material behavior by means of rheological networks.

⁸ The signum function is defined as: $\operatorname{sgn}(a) = \begin{cases} +1 & \text{for } a > 0 \\ 0 & \text{for } a = 0 \\ -1 & \text{for } a < 0 \end{cases}$.

Table 1 Well-known basic elements with stress relation and stored free energy ψ

Linear elastic spring (HOOKE's body "H")	Linear viscous dashpot (NEWTON's body "N")	Friction element ^a (ST.-VENANT's body "ST.-V.")
		
$\sigma = E \varepsilon$	$\sigma = \eta \dot{\varepsilon}$	$\sigma = \kappa_0 \operatorname{sgn}(\dot{\varepsilon})$ for $\dot{\varepsilon} \neq 0$ $ \sigma < \kappa_0$ for $\dot{\varepsilon} = 0$
$\psi = \frac{1}{2\rho} E \varepsilon^2$	$\psi = 0$	$\psi = 0$

^a See also supplemental remark in Appendix A.1

Table 2 Strain and stress relations of series (*left*) and parallel connection (*right*) of two basic elements E_1 and E_2 including structural formula (see Appendix A.2) for resulting substitute element E_3

Series connection	Parallel connection
	
$\varepsilon = \varepsilon_1 + \varepsilon_2$	$\varepsilon = \varepsilon_1 = \varepsilon_2$
$\sigma = \sigma_1 = \sigma_2$	$\sigma = \sigma_1 + \sigma_2$
$E_3 := E_1 - E_2$	$E_3 := E_1 E_2$

The specific mechanical work, applied to the basic elements, according to

$$w = \frac{1}{\rho} \int_0^t \sigma \dot{\varepsilon} d\tau, \tag{27}$$

is either stored as free energy ψ in a particular component or dissipated as heat.

3.1 Classical rheological bodies and element assemblages

In Table 1, the well-known rheological elements according to Reiner [31] are recalled including the associated stress relations and the specific free energy ψ stored in the ideal bodies. New ideal bodies with more complex properties can be generated by assemblages in series and parallel of the basic elements as summarized in Table 2.

3.2 Examples of rheological models for various classes of material behavior

Figure 2 shows simple rheological networks to describe the fundamental material behavior of the model classes, presented in Fig. 1. Elasticity is represented by a linear spring. To illustrate viscoelasticity, a linear spring is combined with a KELVIN element (parallel connection of linear dashpot and linear spring), leading to the three-parameter model of the standard linear solid.

A simple rheological model of elastoplasticity results from the standard linear solid body by replacing the linear dashpot with a friction element. The friction body affects the initial yield stress and may represent isotropic hardening as well, while the spring with stiffness E_ξ allows for modeling of kinematic hardening. Furthermore, a rheological network of elastoviscoplasticity is generated by adding a linear dashpot to the model

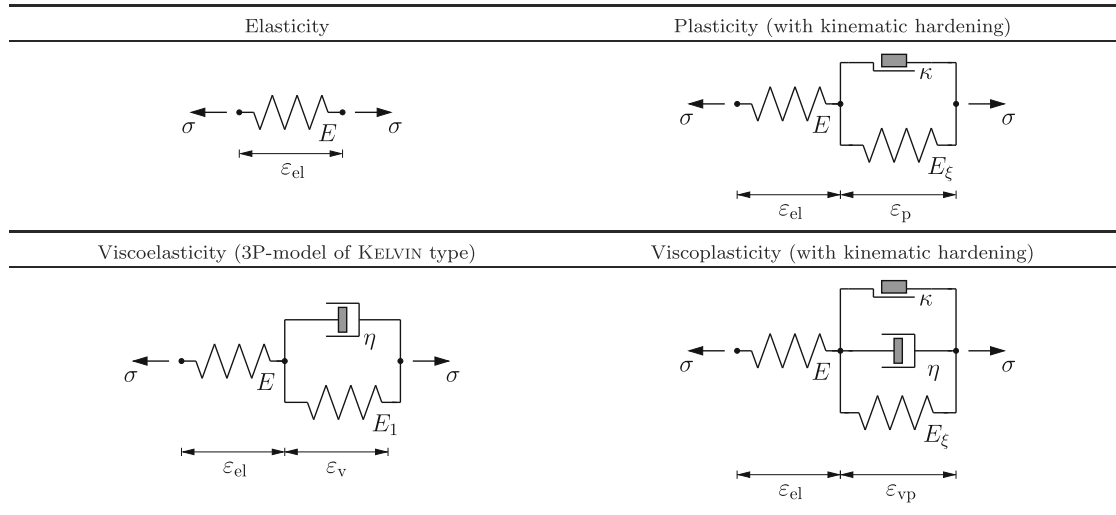


Fig. 2 Rheological models for material behavior specified in Fig. 1

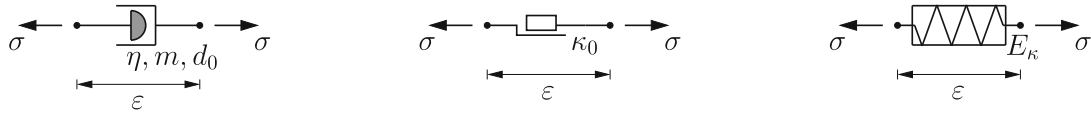


Fig. 3 Nonlinear viscous dashpot with parameters η, m, d_0 (left), modified friction element with energy storage and yield stress κ_0 (center), hardening element with stiffness E_κ (right)

of elastoplasticity, as shown in Fig. 2. Further rheological bodies, found in the literature, are summarized in Appendix A.2.

3.3 Introduction of new or modified rheological elements

3.3.1 Nonlinear viscous dashpot

The stress in the nonlinear viscous dashpot (Fig. 3, left) is initially defined in a general form as

$$\sigma := d(\dot{\bar{\varepsilon}}) \operatorname{sgn}(\dot{\bar{\varepsilon}}), \quad (28)$$

where $d(\dot{\bar{\varepsilon}})$ stands for the absolute value of the dashpot stress as a function of the rate of the arclength $\bar{\varepsilon}$ in this element. In the next step, the function $d(\dot{\bar{\varepsilon}})$ is specified as

$$d(\dot{\bar{\varepsilon}}) := (\eta |\dot{\bar{\varepsilon}}|)^{1/m} d_0, \quad (29)$$

where the parameter η is a positive strain rate scaling factor with the dimension of time. The exponent $1/m$ causes nonlinear rate dependency. However, the additional positive material parameter d_0 introduces stress units, since the term in brackets in (29) is dimensionless. The total work in the nonlinear dashpot is completely dissipated as heat.

3.3.2 Modified friction element with energy storage

The entire mechanical work, spent on the modified friction element, is stored as free energy, which, however, stands in contrast to the classical approach, where a purely dissipative behavior is assigned to this rheological component. With the stress definition for the friction body in Table 1, the associated stored free energy ψ results from (27) with (26) and (24) as proportional to the arclength $\bar{\varepsilon}$ of the strain in this element:

$$\psi = \frac{1}{\rho} \int_0^t \kappa_0 \operatorname{sgn}(\dot{\bar{\varepsilon}}) \dot{\bar{\varepsilon}} \, d\tau = \frac{1}{\rho} \kappa_0 \bar{\varepsilon}. \quad (30)$$



Fig. 4 Dissipative strain element with material parameters c_i (left), thermal strain element with expansion coefficient α (right)

In the graphical representations, for example, in Fig. 3 (center), the rectangle of the modified friction body⁹ remains transparent to differ it from its dissipative counterpart, specified in Table 1.

3.3.3 Hardening element

The novel element for modeling isotropic hardening (Fig. 3, right) has to respond to the strain process with an increasing resistance to plastic flow, however, without reducing its new gained strength after load reversal, as occurring in models of kinematic hardening by means of a simple spring. Following this aspect, a linear relationship

$$|\sigma| := E_\kappa \varepsilon_\kappa \quad (31)$$

is most obvious, where E_κ is a stiffness-like parameter and ε_κ specifies a monotonously growing internal variable of strain type, determined by the evolution equation

$$\dot{\varepsilon}_\kappa := |\dot{\varepsilon}|. \quad (32)$$

By using the definition (24), the time integration of (32) yields the absolute value of the stress (31) as

$$|\sigma| = E_\kappa \bar{\varepsilon} \quad (33)$$

with the arclength $\bar{\varepsilon}$ of the strain ε . During the loading process $\dot{\varepsilon} \neq 0$, the algebraic sign of the stress σ has to correspond to the strain rate $\dot{\varepsilon}$ in the hardening body:

$$\text{sgn}(\sigma) = \text{sgn}(\dot{\varepsilon}). \quad (34)$$

However, as long as the absolute value of the stress σ in the element is less than its actual strength $E_\kappa \bar{\varepsilon}$, no strains may evolve in this rheological component. Hence, the total stress of the hardening element reads as

$$\begin{aligned} \sigma &= E_\kappa \bar{\varepsilon} \text{sgn}(\dot{\varepsilon}) & \text{for } \dot{\varepsilon} \neq 0 \\ |\sigma| &< E_\kappa \bar{\varepsilon} & \text{for } \dot{\varepsilon} = 0 \end{aligned} \quad (35)$$

with a case distinction similar to the one of the friction body in Table 1.

It is postulated that all work, applied to the hardening element, is stored as free energy. Thus, (27) leads to the free energy term

$$\psi = \frac{1}{\rho} \int_0^t E_\kappa \bar{\varepsilon} \text{sgn}(\dot{\varepsilon}) \dot{\varepsilon} \, d\tau = \frac{1}{\rho} \int_0^{\bar{\varepsilon}} E_\kappa \bar{\varepsilon} \, d\bar{\varepsilon} = \frac{1}{2\rho} E_\kappa \bar{\varepsilon}^2, \quad (36)$$

exhibiting a structure very similar to the corresponding expression of the stored energy in a linear elastic spring as given in Table 1.

⁹ Subsequently, the term friction element always refers to the modified type introduced here, unless indicated differently.

3.3.4 Dissipative strain element

The dissipative strain element¹⁰ (Fig. 4, left) is used to limit the strain part and, thus, the stored free energy evolving in other ideal bodies such as the hardening elements embedded in the rheological network. The work, applied in this process to the dissipative strain element, is completely transferred into heat. The stress σ in this ideal dissipation body shall not depend on its actual strain value ε , since this rheological component only transfers the external stress σ . However, the strain, emerging in the dissipative strain element, is controlled solely by an evolution equation

$$\dot{\varepsilon} := \zeta(\varepsilon, \sigma, a_j, \dots), \quad (37)$$

which may be introduced as a function of the strain ε , the stress σ and further internal or external variables a_j as well as the associated material parameters c_i . Later on when the material model is set up, a reasonable definition must be given to the evolution equation (37) in each application of the dissipative strain element.

3.3.5 Thermal strain element

The thermal strain element (Fig. 4, right) responds like a rigid body to every mechanical loading due to external forces or displacements. However, under temperature changes with respect to the reference level θ_0 , a thermal strain ε_{th} develops in the element according to

$$\varepsilon_{\text{th}} = \alpha(\theta - \theta_0), \quad (38)$$

that is, the thermal strain rate is recovered as assumed in (3). The free energy, specified for the thermal strain element—see Appendix A.3, is given by

$$\psi = -\frac{1}{2\theta_0} c_{\text{def}}(\theta - \theta_0)^2. \quad (39)$$

4 Enhanced rheological model of thermoviscoplasticity

The enhanced rheological model of thermoviscoplasticity (Fig. 5) consists of two parts: the thermoelastic contribution on the left-hand side, comprising a thermal strain element and a linear spring, as well as the considerably more complex viscoplastic model composition on the right. This assemblage consists of four chains arranged in parallel, each one representing a specific phenomenon of the entire elastoviscoplastic material response.

The first branch on top with the nonlinear dashpot is for the representation of the velocity-related overstress effect [20] in the material model. In the second chain of the parallel network assemblage, a friction body and a dissipative strain element are arranged in series to account for elastoplastic behavior with the initial yield stress and to improve the energy transformation characteristic of the resulting material model during plastic flow. In the third chain, a hardening element is connected in series to a dissipative strain element for realizing nonlinear isotropic hardening and energy diffusion. The fourth chain of the rheological model finally includes a linear spring with a dissipative strain element for describing nonlinear kinematic hardening¹¹.

The difference between dissipative and energy storing components is marked graphically in the rheological network: The gray colored areas indicate the dissipative character of the dashpot and the dissipative strain bodies. In all other elements, solely energy storage takes place.

¹⁰ A kind of dissipative strain element—however, not denoted with this expression—was introduced firstly by Krawietz [19] as part of a rheological model to describe endochronic plasticity. In the following this rheological component is generalized into a dissipative strain element.

¹¹ A simplified version of the rheological model with linear hardening is briefly discussed in [4], comprising a dissipative friction body but none dissipative strain elements.

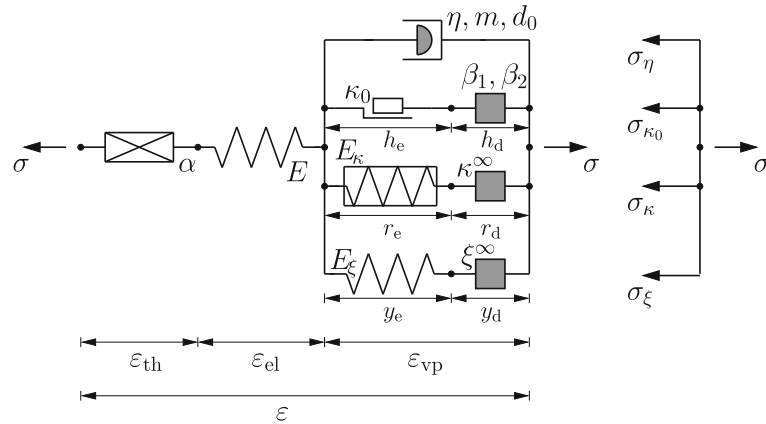


Fig. 5 Enhanced rheological model of thermoviscoplasticity with nonlinear isotropic and kinematic hardening and improved description of energy storage and dissipation

4.1 Kinematics, internal stresses and free energy

The kinematics of the rheological model in Fig. 5 results from the network rules for the basic elements in series and parallel connection in Table 2. It gives the relation between the total strain ε and the thermal, the elastic, and the viscoplastic strain fractions:

$$\varepsilon = \varepsilon_{th} + \varepsilon_{el} + \varepsilon_{vp}. \quad (40)$$

A further additive decomposition of the viscoplastic strain and its rate follows from the four chains in the viscoplastic part of the model according to

$$\varepsilon_{vp} = h_e + h_d = r_e + r_d = y_e + y_d \quad (41)$$

and

$$\dot{\varepsilon}_{vp} = \dot{h}_e + \dot{h}_d = \dot{r}_e + \dot{r}_d = \dot{y}_e + \dot{y}_d. \quad (42)$$

The indices “e” and “d” denote the elastic or energy storing and the dissipative character of the internal strain variables.

Moreover, the rheological model provides an additive decomposition of the total stress into the partial stresses in the parallel chains for viscoplasticity:

$$\sigma = \sigma_\eta + \sigma_{\kappa_0} + \sigma_\kappa + \sigma_\xi, \quad (43)$$

which stem from the corresponding definitions of the basic elements in (28), (35) as well as in table 1 and are given by the following material equations:

$$\sigma_\eta = d(\dot{\varepsilon}_{vp}) \operatorname{sgn}(\dot{\varepsilon}_{vp}) \quad \text{nonlinear viscous dashpot} \quad (44)$$

$$\sigma_{\kappa_0} = \kappa_0 \operatorname{sgn}(\dot{h}_e) \quad \text{for } \dot{h}_e \neq 0 \quad \text{friction element} \quad (45)$$

$$|\sigma_{\kappa_0}| < \kappa_0 \quad \text{for } \dot{h}_e = 0 \quad (46)$$

$$\sigma_\kappa = E_\kappa \bar{r}_e \operatorname{sgn}(\dot{r}_e) =: \kappa \operatorname{sgn}(\dot{r}_e) \quad \text{for } \dot{r}_e \neq 0 \quad \text{hardening element} \quad (47)$$

$$|\sigma_\kappa| < E_\kappa \bar{r}_e = \kappa \quad \text{for } \dot{r}_e = 0 \quad (48)$$

$$\sigma_\xi = E_\xi y_e =: \xi \quad \text{spring of kin. hardening} \quad (49)$$

The quantity $\kappa = E_\kappa \bar{r}_e$ represents the stress of isotropic hardening and ξ is the kinematic hardening variable of stress type.

The free energy ψ of the rheological model follows from all basic elements contributing to energy storage:

$$\psi = \psi_{\text{th}} + \psi_{\text{el}} + \psi_{\kappa_0} + \psi_{\kappa} + \psi_{\xi}, \quad (50)$$

that is, from the energy contributions of the thermal strain element ψ_{th} and the linear spring ψ_{el} in the thermoelastic part according to the definitions in (39) and Table 1 as well as from the friction element ψ_{κ_0} , the hardening element ψ_{κ} , and the spring ψ_{ξ} for kinematic hardening in the viscoplastic part according to (30, 36) and Table 1. It may be summarized as

$$\psi = \psi(\varepsilon_{\text{el}}, \theta, \bar{h}_e, \bar{r}_e, y_e) = \frac{1}{\rho} \left[\frac{1}{2} E \varepsilon_{\text{el}}^2 - \frac{1}{2\theta_0} \rho c_{\text{def}} (\theta - \theta_0)^2 + \kappa_0 \bar{h}_e + \frac{1}{2} E_{\kappa} \bar{r}_e^2 + \frac{1}{2} E_{\xi} y_e^2 \right]. \quad (51)$$

4.2 Implications from mechanical dissipation

With the free energy ψ as in (51)₁, the inequality of the mechanical dissipation (13) becomes

$$\delta_{\text{M}} = \frac{1}{\rho} \sigma \dot{\varepsilon}_{\text{vp}} - \frac{\partial \psi}{\partial \bar{h}_e} \dot{\bar{h}}_e - \frac{\partial \psi}{\partial \bar{r}_e} \dot{\bar{r}}_e - \frac{\partial \psi}{\partial y_e} \dot{y}_e \geq 0. \quad (52)$$

By substituting the kinematical assumption (42) and the balance equation of stresses (43) into the first term of (52), the viscoplastic stress power is decomposed similarly as in [23] into the contributions of the individual elements:

$$\frac{1}{\rho} \sigma \dot{\varepsilon}_{\text{vp}} = \frac{1}{\rho} \left[\sigma_{\eta} \dot{\varepsilon}_{\text{vp}} + \sigma_{\kappa_0} (\dot{h}_e + \dot{h}_d) + \sigma_{\kappa} (\dot{r}_e + \dot{r}_d) + \sigma_{\xi} (\dot{y}_e + \dot{y}_d) \right]. \quad (53)$$

In order to evaluate the expression in (53), the component stresses (44, 45, 47) and (49) of the basic elements are inserted into the viscoplastic stress power¹²:

$$\frac{1}{\rho} \sigma \dot{\varepsilon}_{\text{vp}} = \frac{1}{\rho} \left[d(\dot{\varepsilon}_{\text{vp}}) \text{sgn}(\dot{\varepsilon}_{\text{vp}}) \dot{\varepsilon}_{\text{vp}} + \kappa_0 \text{sgn}(\dot{h}_e) (\dot{h}_e + \dot{h}_d) + \kappa \text{sgn}(\dot{r}_e) (\dot{r}_e + \dot{r}_d) + \xi (\dot{y}_e + \dot{y}_d) \right]. \quad (54)$$

Applying the identity (26) for the first, second and third summand in (54) as well as the rule $\text{sgn}(a) \cdot \text{sgn}(a) = 1$ yields the following:

$$\frac{1}{\rho} \sigma \dot{\varepsilon}_{\text{vp}} = \frac{1}{\rho} \left(d(\dot{\varepsilon}_{\text{vp}}) \dot{\varepsilon}_{\text{vp}} + \kappa_0 \dot{\bar{h}}_e + \kappa_0 \text{sgn}(\dot{h}_e) \dot{h}_d + \kappa \dot{\bar{r}}_e + \kappa \text{sgn}(\dot{r}_e) \dot{r}_d + \xi \dot{y}_e + \xi \dot{y}_d \right). \quad (55)$$

Thus, by using the decomposition (55), the dissipation inequality (52) generates the intermediate result:

$$\begin{aligned} \delta_{\text{M}} = \frac{1}{\rho} \left[d(\dot{\varepsilon}_{\text{vp}}) \dot{\varepsilon}_{\text{vp}} + \left(\kappa_0 - \rho \frac{\partial \psi}{\partial \bar{h}_e} \right) \dot{\bar{h}}_e + \left(\kappa - \rho \frac{\partial \psi}{\partial \bar{r}_e} \right) \dot{\bar{r}}_e + \left(\xi - \rho \frac{\partial \psi}{\partial y_e} \right) \dot{y}_e \right. \\ \left. + \kappa_0 \text{sgn}(\dot{h}_e) \dot{h}_d + \kappa \text{sgn}(\dot{r}_e) \dot{r}_d + \xi \dot{y}_d \right] \geq 0. \end{aligned} \quad (56)$$

Each summand in (56) is inspected separately, starting with the rate terms of the internal strain variables $\dot{\bar{h}}_e$, $\dot{\bar{r}}_e$ and \dot{y}_e . The rate \dot{y}_e can be positive, zero or negative, whereas the rates $\dot{\bar{h}}_e$ and $\dot{\bar{r}}_e$ are always semipositive. However, the absolute values of all these rates may tend toward infinity, while the associated factors within the round brackets in (56) may be negative as well. Semipositivity of the mechanical dissipation (56) may only be guaranteed for all conceivable states of the internal strain rates, if both prefactors of the rates $\dot{\bar{h}}_e$ and $\dot{\bar{r}}_e$ are at least semipositive and, furthermore, the factor ahead of the rate \dot{y}_e vanishes identically. Hence, it is more strictly demanded as only sufficient conditions that all three terms in round brackets in (56) have to be identical zero at all points in time during the entire strain process. Assuring that the prefactors of the internal

¹² In fact, the component stresses of the friction and the hardening element (45) to (48) require the investigation of four different cases. However, exclusively, the case with the relations (45) and (47) is considered subsequently, that is, $\dot{h}_e \neq 0$ and $\dot{r}_e \neq 0$ hold for the following steps.

strain rates itself are independent of \dot{h}_e , \dot{r}_e and \dot{y}_e , three additional potential relations of the free energy result for the internal stress variables as sufficient but not necessary conditions:

$$\kappa_0 = \rho \frac{\partial \psi}{\partial \bar{h}_e}, \quad (57)$$

$$\kappa = \rho \frac{\partial \psi}{\partial \bar{r}_e}, \quad (58)$$

$$\xi = \rho \frac{\partial \psi}{\partial y_e}, \quad (59)$$

leaving the reduced mechanical dissipation as the remaining inequality according to

$$\delta_M = \frac{1}{\rho} \left(d(\dot{\bar{\epsilon}}_{vp}) \dot{\bar{\epsilon}}_{vp} + \kappa_0 \operatorname{sgn}(\dot{h}_e) \dot{h}_d + \kappa \operatorname{sgn}(\dot{r}_e) \dot{r}_d + \xi \dot{y}_d \right) \geq 0. \quad (60)$$

In accordance with the second law of thermomechanics, the stricter requirement is posed onto the inequality (60) that each summand by itself has to be nonnegative. As a consequence of the definitions for the dashpot stress (28) and the arlength (25), the first summand in (60) is positive in any case. The remaining three terms in (60) provide the following conclusions for the evolution equations of the internal strain variables

$$\operatorname{sgn}(\dot{h}_d) = \operatorname{sgn}(\dot{h}_e) \quad \text{or} \quad \dot{h}_d = 0 \Rightarrow \dot{h}_e = \dot{\bar{\epsilon}}_{vp}, \quad (61)$$

$$\operatorname{sgn}(\dot{r}_d) = \operatorname{sgn}(\dot{r}_e) \quad \text{or} \quad \dot{r}_d = 0 \Rightarrow \dot{r}_e = \dot{\bar{\epsilon}}_{vp}, \quad (62)$$

$$\operatorname{sgn}(\dot{y}_d) = \operatorname{sgn}(\xi) \quad \text{or} \quad \dot{y}_d = 0 \Rightarrow \dot{y}_e = \dot{\bar{\epsilon}}_{vp} \quad (63)$$

as sufficient condition to assure semipositivity of the mechanical dissipation and to satisfy (42)₁ to (42)₃. However, the latter relations of (61) to (63) specify trivial cases of the rheological network, in which no strains may evolve in the dissipative strain elements. For this reason, these cases are not investigated any further. With the relation (26)₂, it follows from the decomposition of the viscoplastic strain rate $\dot{\bar{\epsilon}}_{vp}$ according to (42)₁ and (42)₂ as well as from (61)₁ and (62)₁ that

$$\dot{\bar{\epsilon}}_{vp} = \dot{\bar{\epsilon}}_{vp} \operatorname{sgn}(\dot{\bar{\epsilon}}_{vp}) = \dot{h}_e \operatorname{sgn}(\dot{h}_e) + \dot{h}_d \operatorname{sgn}(\dot{h}_d) = \left(\dot{h}_e + \dot{h}_d \right) \operatorname{sgn}(\dot{h}_d) = \left(\dot{r}_e + \dot{r}_d \right) \operatorname{sgn}(\dot{r}_d) \quad (64)$$

holds. Hence, the internal strains in the chains of the friction and hardening element develop in the same direction as the viscoplastic strain rate does:

$$\operatorname{sgn}(\dot{\bar{\epsilon}}_{vp}) = \operatorname{sgn}(\dot{h}_d) = \operatorname{sgn}(\dot{h}_e) = \operatorname{sgn}(\dot{r}_d) = \operatorname{sgn}(\dot{r}_e) \neq 0. \quad (65)$$

Note that the unequal sign results at the end of (65) since (54) is valid only for $\dot{h}_e \neq 0$ and $\dot{r}_e \neq 0$ —see footnote 12. Moreover, according to (64), the rate of the viscoplastic strain functional $\bar{\epsilon}_{vp}$ decomposes into the parts of the friction or hardening body and the dissipative strain elements attached:

$$\dot{\bar{\epsilon}}_{vp} = \dot{h}_e + \dot{h}_d = \dot{r}_e + \dot{r}_d. \quad (66)$$

As a further consequence of (66) and the definition (24)₂, the viscoplastic arlength $\bar{\epsilon}_{vp}$ boils down according to

$$\bar{\epsilon}_{vp} = \int_0^t \dot{\bar{\epsilon}}_{vp}(\tau) d\tau = \int_0^t \left(\dot{h}_e(\tau) + \dot{h}_d(\tau) \right) d\tau = \int_0^t \dot{h}_e(\tau) d\tau + \int_0^t \dot{h}_d(\tau) d\tau = \bar{h}_e + \bar{h}_d \quad (67)$$

into the fractions of the partial strains

$$\bar{\epsilon}_{vp} = \bar{h}_e + \bar{h}_d = \bar{r}_e + \bar{r}_d, \quad (68)$$

which is equivalent to the decomposition in (66). Finally, the mechanical dissipation (60) is transferred with the equalities (61)₁, (62)₁ and (63)₁ as well as the relation (26)₂ for the strain rates \dot{h}_d and \dot{r}_d into the semipositive expression

$$\delta_M = \frac{1}{\rho} \left(d(\dot{\bar{\varepsilon}}_{vp}) \dot{\bar{\varepsilon}}_{vp} + \kappa_0 \dot{h}_d + \kappa \dot{r}_d + |\xi| \dot{\bar{y}}_d \right). \quad (69)$$

Its four summands can be directly assigned to the dissipative components in the rheological model of Fig. 5. The first term comprises the stress power, dissipated in the dashpot. The other three contributions correspond to the stress power of the dissipative strain elements, connected in series to the friction and the isotropic hardening body as well as to the spring of kinematic hardening.

4.3 Evolution equation of dissipative strain element

4.3.1 Evolution of internal strain h_d

The sign of the internal strain rate \dot{h}_d in the dissipative strain element has already been discussed in (65), but a suitable equation for the rate of the arclength \dot{h}_d is provided next. According to (51) and (66), the energy storing rate in the friction body becomes

$$\dot{\psi}_{\kappa_0} = \frac{1}{\rho} \kappa_0 \dot{h}_e = \frac{1}{\rho} \kappa_0 \left(\dot{\bar{\varepsilon}}_{vp} - \dot{h}_d \right). \quad (70)$$

As found by experimental investigations [7, 13, 28, 29], the rate of energy storage in the friction element $\dot{\psi}_{\kappa_0}$ has to be large in the beginning of the plastic process. But as plastification increases, the energy storing rate $\dot{\psi}_{\kappa_0}$ has to reduce and should finally tend to zero. With respect to the kinematics of the rheological model this means: Initially, mainly the strain h_e in the friction body develops, causing energy storage, whereas the strain h_d in the dissipative strain component remains small. However, in the course of plastic loading, the development of h_e diminishes in favor of larger strain rates \dot{h}_d , until finally the evolution of h_e reaches a state of complete saturation, that is, the rate in the dissipative strain element is approximately equal to the viscoplastic strain rate $\dot{h}_d \approx \dot{\bar{\varepsilon}}_{vp}$, whereas the strain rate \dot{h}_e in the friction body tends to zero with time.

A suitable evolution equation for the internal variable h_d , allowing for the afore outlined properties, is proposed as a function of the monotonically increasing viscoplastic arclength $\bar{\varepsilon}_{vp}$ and with respect to the constraint (65) according to

$$\dot{h}_d = \left(1 - \beta_1 e^{-\beta_2 \bar{\varepsilon}_{vp}} \right) \dot{\bar{\varepsilon}}_{vp} \quad (71)$$

with the parameters $0 \leq \beta_1 \leq 1$ and $\beta_2 \geq 0$. The initial and long-term rates of energy storage in the friction body are given by $\dot{\psi}_{\kappa_0}(\bar{\varepsilon}_{vp} = 0) = \frac{1}{\rho} \kappa_0 \dot{\bar{\varepsilon}}_{vp} \beta_1$ and $\dot{\psi}_{\kappa_0}(\bar{\varepsilon}_{vp} \rightarrow \infty) = 0$. Choosing $\beta_2 = 0$ results in a constant energy storing rate in the friction element, which corresponds to the approach of Helm [13, 14] for ideal plasticity and to the one of Chaboche [6], denoted as ‘‘saturated isotropic hardening.’’

4.3.2 Evolution of internal strain r_d and isotropic hardening stress κ

The rheological model at hand shall represent nonlinear isotropic hardening. According to the material equation for the stress in the hardening element (47), the related internal variable κ of stress type is linear in the arclength \bar{r}_e . Thus, as in the friction body, mainly the internal strain r_e has to grow at the beginning of plastic loading. But with increasing strength κ , the strain rate \dot{r}_e in the hardening body has to diminish during plastic flow in favor of a larger rate \dot{r}_d in the associated dissipative strain component until saturation of the isotropic hardening variable κ is finally approached, that is, $\dot{r}_d \approx \dot{\bar{\varepsilon}}_{vp}$ holds. Ensuring the validity of the constraint (65), an evolution equation for r_d is set as linear in the product of the viscoplastic strain rate and the internal stress variable κ :

$$\dot{r}_d = \frac{\kappa}{\kappa_\infty} \dot{\bar{\varepsilon}}_{vp}, \quad (72)$$

where the positive material parameter κ^∞ corresponds to the saturation value of the isotropic hardening stress. With (47) and (66) as well as (72), the evolution equation of the isotropic hardening variable κ follows as

$$\dot{\kappa} = E_\kappa (\dot{\hat{\epsilon}}_{vp} - \dot{\hat{r}}_d) = E_\kappa \left(1 - \frac{\kappa}{\kappa^\infty}\right) \dot{\hat{\epsilon}}_{vp}. \quad (73)$$

Linear isotropic hardening is recovered for the internal variable $\dot{\hat{r}}_d \equiv 0$ as a special case.

4.3.3 Evolution of internal strain y_d and kinematic hardening stress ξ

During monotonic loading, the kinematical requirements on the internal strains y_e and y_d for nonlinear kinematic hardening are similar to their counterparts r_e and r_d for the increase of isotropic strength κ discussed above. However, in contrast to κ , the kinematic hardening variable $\xi = E_\xi y_e$ has to diminish rapidly in the case of load reversal, and after passing through zero, it has to develop with the opposite algebraic sign up to the point of saturation in the opposed direction. Searching for a suitable evolution equation for the internal strain y_d , which allows for the outlined hardening behavior, the constraint (63)₁ already governs the direction of evolution and, thus, motivates a linear relationship, similar to (72), in terms of the internal stress variable ξ :

$$\dot{y}_d = \frac{\xi}{\xi^\infty} \dot{\hat{\epsilon}}_{vp}, \quad (74)$$

where the positive material parameter ξ^∞ corresponds to the absolute value of the kinematic hardening stress ξ at the state of complete saturation. By using (42), the rate of the internal strain y_e , inducing the stress $\xi = E_\xi y_e$ due to the kinematic hardening, results as

$$\dot{y}_e = \dot{\hat{\epsilon}}_{vp} - \dot{y}_d = \dot{\hat{\epsilon}}_{vp} - \frac{\xi}{\xi^\infty} \dot{\hat{\epsilon}}_{vp} = \left(1 - \frac{|\xi|}{\xi^\infty} \operatorname{sgn}(\xi) \operatorname{sgn}(\dot{\hat{\epsilon}}_{vp})\right) \dot{\hat{\epsilon}}_{vp}. \quad (75)$$

During monotonic tensile loading, the qualitative evolution of both internal strain rates \dot{y}_e and \dot{y}_d is identical as for the rates \dot{r}_e and \dot{r}_d of isotropic hardening before. However, in the case of load reversal, the term in the brackets of (75)₃ has an initial value of 2—that is, the rate of the internal strain y_e is initially twice as high as the viscoplastic strain rate $\dot{\hat{\epsilon}}_{vp}$ itself, which at first causes a very strong reduction in the kinematic hardening variable ξ and, hence, also the decrease in the rate of strain y_d in the dissipation element. However, according to (74), the strain y_d still augments with the identical algebraic sign as before the change of the loading direction as long as the hardening stress ξ is positive. When the internal strain y_e and the kinematic hardening variable ξ become negative for the first time, also the algebraic sign of the rate \dot{y}_d in (74) inverts, and hence, the development of the strain y_e and the kinematic hardening variable ξ slows down. In the following, the ratio ξ/ξ^∞ tends to -1 and the internal strain y_e saturates in the negative range of values¹³.

Equation (49) with (75) finally leads to the evolution equation of nonlinear kinematic hardening according to

$$\dot{\xi} = E_\xi \dot{y}_e = E_\xi \left(\dot{\hat{\epsilon}}_{vp} - \frac{\xi}{\xi^\infty} \dot{\hat{\epsilon}}_{vp}\right) \quad (76)$$

and, thus, corresponds to the approach of Armstrong and Frederick [2]. In the special case $\dot{y}_d \equiv 0$ of the vanishing internal strain variable y_d , the kinematic hardening is only linear.

4.4 Yield condition and flow rule

The balance equation of stresses (43) is transformed by means of the component stresses (44, 45, 47) and (49) as well as by the relation of the evolution directions (65) into¹⁴

$$\sigma = d(\dot{\hat{\epsilon}}_{vp}) \operatorname{sgn}(\dot{\hat{\epsilon}}_{vp}) + \kappa_0 \operatorname{sgn}(\dot{\hat{\epsilon}}_{vp}) + \kappa \operatorname{sgn}(\dot{\hat{\epsilon}}_{vp}) + \xi. \quad (77)$$

¹³ If another load reversal is applied, then the development of the internal strains repeats in an analogous way as discussed above, but each one with its opposite algebraic sign.

¹⁴ It is assumed temporarily for the stress balance (43) that the stress relations (45) and (47) of the friction and the hardening body are valid in any case, which, in consequence of (65), is equivalent to the tentative hypothesis: *Only elastoviscoplastic states are possible in the rheological network, that is, $\dot{\hat{\epsilon}}_{vp} \neq 0$ and $\operatorname{sgn}(\dot{\hat{\epsilon}}_{vp}) = \operatorname{sgn}(\dot{h}_e) = \operatorname{sgn}(\dot{r}_e) \neq 0$ hold for any time and no purely elastic domain exists.* However, this assumption causes a mathematical contradiction as soon as purely elastic behavior occurs. In this manner, the condition emerges to distinguish between the elastic and plastic state of the model.

Rewriting of (77) leads to

$$\sigma - \xi = |\sigma - \xi| \operatorname{sgn}(\sigma - \xi) = \left(d(\dot{\varepsilon}_{\text{vp}}) + \kappa_0 + \kappa \right) \operatorname{sgn}(\dot{\varepsilon}_{\text{vp}}). \quad (78)$$

According to the defining relations for the dashpot (29) and the friction element (Table 1) as well as to the one for the internal stress κ in (47), all summands in the bracket on the right-hand side of (78) are strictly positive. As the algebraic signs of the terms $\operatorname{sgn}(\sigma - \xi) = \operatorname{sgn}(\dot{\varepsilon}_{\text{vp}})$ must be equal, (78) provides the constitutive relation for the absolute value of the overstress in the dashpot

$$d(\dot{\varepsilon}_{\text{vp}}) = |\sigma - \xi| - (\kappa_0 + \kappa). \quad (79)$$

By introducing the function $f := |\sigma - \xi| - (\kappa_0 + \kappa)$ into (79), it follows

$$d(\dot{\varepsilon}_{\text{vp}}) = f. \quad (80)$$

The equal sign in (80) can only be valid, if the function f is semipositive. However, dependent on the actual state of the total and the internal stress variables σ , ξ , κ and κ_0 , the function f can have negative values as well. The mathematical contradiction in (80) in the case of $f < 0$ indicates that no plastic loading is possible in the rheological model for all states $f < 0$ —see also footnote 14. Instead, a purely thermoelastic step takes place, that is, $\dot{\varepsilon}_{\text{vp}} = 0$ holds. Moreover, in the case of $f < 0$, the stress relations (46) and (48) of the friction and the hardening body are valid in lieu of (45) and (47). Thus, the well-known yield function

$$f = |\sigma - \xi| - (\kappa_0 + \kappa) \quad (81)$$

with the case distinctions

$$f = \begin{cases} \leq 0 & \text{elastic domain} \\ > 0 & \text{viscoplastic domain} \end{cases} \quad (82)$$

arises naturally from the rheological network. Indeed, (77) to (80) are valid only for states $f \geq 0$ of total and internal stresses σ , κ_0 , κ and ξ . Hence, solely values with $f \geq 0$ must be allowed for in (80), which may be mathematically realized by means of the Macauley bracket $\langle x \rangle := (x + |x|)/2$. Thus, (80) is transferred with the definition of the dashpot stress (29) into

$$d(\dot{\varepsilon}_{\text{vp}}) = (\eta |\dot{\varepsilon}_{\text{vp}}|)^{1/m} d_0 = \langle f \rangle. \quad (83)$$

If f is negative, then the right-hand side of (83) is zero, which directly leads to $|\dot{\varepsilon}_{\text{vp}}| = 0$ and, thus, reveals that viscoplastic strains ε_{vp} do not evolve in the rheological network for nonpositive values $f \leq 0$. That means, the thermoelastic part of the model is active only. Inelastic strains, however, only develop in case $f > 0$. Rearranging (83) brings the absolute value of the viscoplastic strain rate into the form

$$|\dot{\varepsilon}_{\text{vp}}| = \frac{1}{\eta} \left\langle \frac{f}{d_0} \right\rangle^m =: \lambda, \quad (84)$$

which is equal to the plastic multiplier λ according to the approach of Perzyna [30]. After use is made of (84) and the algebraic sign from (78), the flow rule of the viscoplastic strain reads¹⁵

$$\dot{\varepsilon}_{\text{vp}} = \frac{1}{\eta} \left\langle \frac{f}{d_0} \right\rangle^m \frac{\sigma - \xi}{|\sigma - \xi|}. \quad (85)$$

¹⁵ The sign of the viscoplastic strain rate, as given by (78), corresponds to the known normal direction of the associated theory of rate-independent plasticity: $\operatorname{sgn}(\dot{\varepsilon}_{\text{vp}}) \equiv \partial f / \partial \sigma$.

4.5 Equation of heat conduction

According to the potential relations (6) and (7), the stress and entropy follow from the free energy (51)₂ as

$$\sigma = E\varepsilon_{\text{el}}, \quad s = \frac{1}{\rho}E\alpha\varepsilon_{\text{el}} + \frac{1}{\theta_0}c_{\text{def}}(\theta - \theta_0), \quad (86)$$

and the derivatives of the entropy with respect to the elastic and internal strains in the equation of heat conduction (19) read as

$$\frac{\partial s}{\partial \varepsilon_{\text{el}}} = \frac{1}{\rho}E\alpha, \quad \frac{\partial s}{\partial a_j} = 0. \quad (87)$$

Hence, the thermoviscoplastic coupling term p_i in (19) vanishes as a consequence of the free energy expression in (51)₂. The mechanical dissipation (69) follows with the help of the evolution equations (71, 72) and (74) for the internal strains h_d , r_d and y_d as well as with (83) as¹⁶

$$\delta_M = \frac{1}{\rho} \left[f + \kappa_0 \left(1 - \beta_1 e^{-\beta_2 \bar{\varepsilon}_{\text{vp}}} \right) + \frac{\kappa^2}{\kappa^\infty} + \frac{\xi^2}{\xi^\infty} \right] \dot{\bar{\varepsilon}}_{\text{vp}} \geq 0. \quad (88)$$

The mechanical dissipation (88) is semipositive as required to assure the thermomechanical consistency of the material model¹⁷. Finally, the equation of heat conduction (19) reduces with (87) to

$$c_{\text{def}} \dot{\theta} = -\frac{1}{\rho}E\alpha \theta \dot{\varepsilon}_{\text{el}} + \frac{1}{\rho}k \operatorname{div}(g) + b + \delta_M. \quad (89)$$

Remarks

- The rheological network in Fig. 5 may be reduced to the special cases of rate-independent thermoplasticity as well as to thermoviscoelasticity as discussed in Appendix A.5.
- An additional Appendix A.6 shows the comparison of the energy representation from the rheological model (51)₂ to the classical proposal for the Helmholtz free energy in the theory of thermoelasticity.

5 Model validation for energy transformation

The material model of Sect. 4 is implemented into a one-dimensional truss element of the FE-program FEAP¹⁸. Since the purely mechanical contribution of the constitutive model is quite well-known in the framework of the theory of metal plasticity, less attention is paid in this work to the validation of the mechanical model response and the related identification procedure of the material parameters. Instead, simulations with four different variants of energy storage models are performed—see Table 3—in order to validate the energy transformation characteristic of the material model by means of experimental data in [13]. In this test, a cylindrical specimen, made of AlMgSi, is loaded in tension up to the strain limit $\varepsilon = 4\%$, with a strain rate kept constant at $\dot{\varepsilon} = 0.004 \text{ s}^{-1}$. The stress history is measured and the change of the surface temperature is recorded in the mid-point of the sample. Based on this temperature data, the energy transformation ratio φ (also denoted as ETR) according to (20) is given in [13].

According to the experiment, isothermal boundary conditions are applied in the simulations at both ends of the specimen. The mechanical and thermal material parameters are adopted from the experimental data and the identification of Helm [13] as given in Tables 3 and 4. Kinematic hardening is excluded in these calculations.

The simulated stress response is identical for all models (a–d) and agrees well with the experimental data except toward the end of the test at time $t > 7\text{s}$ —see Fig. 6, left picture. However, the calculated ratios of the energy transformation φ clearly differ from each other (Fig. 7) and, thus, also the calculated temperature histories—see Fig. 6, right picture. The cooling phase with temperature drop at the beginning of the five plots for the temperature history can be attributed to the thermoelastic coupling effect.

¹⁶ Since the factor $\dot{\bar{\varepsilon}}_{\text{vp}}$ in (88) is identically zero all over in the elastic range—see (25) and (84), the Macauley bracket of the yield function f from (83) may be omitted in the first summand of (88).

¹⁷ Two further formulations of the mechanical dissipation δ_M are discussed in Appendix A.4.

¹⁸ Taylor, R.L.: FEAP—A Finite Element Analysis Program, Version 7.5, Theory Manual. University of California at Berkeley, Berkeley, USA, www.ce.berkeley.edu/feap (2003).

Table 3 Parameters of energy storage models

Model	Parameter	Model type
a	$\gamma = 0.9$	Constant ETR as in (23)
b	$\beta_1 = 0.0, \beta_2 = 0.0$	Energy storage due to hardening only ^a
c	$\beta_1 = 0.4, \beta_2 = 0.0$	Model of Helm [13]
d	$\beta_1 = 0.75, \beta_2 = 60.0$	New proposal according to (71)

^a This model type corresponds formally to a rheological network similar to Fig. 5, which has a purely dissipative friction body, however, without a dissipative strain element, arranged in series

Table 4 Further material parameters

Parameter type	Symbol	Value	Symbol	Value	Symbol	Value
Thermoelastic	E	60,759.5 N/mm ²	ρ	2,900.0 kg/m ³	α	2.15×10^{-5} 1/K
	k	210.0 W/(m K)	c_{def}	940.0 J/(kg K)		
Viscoplastic	d_0	1.0 N/mm ²	η	1.0 s	m	1.0
	κ_0	60.0 N/mm ²	E_κ	5,250.0 N/mm ²	κ^∞	61.8 N/mm ²

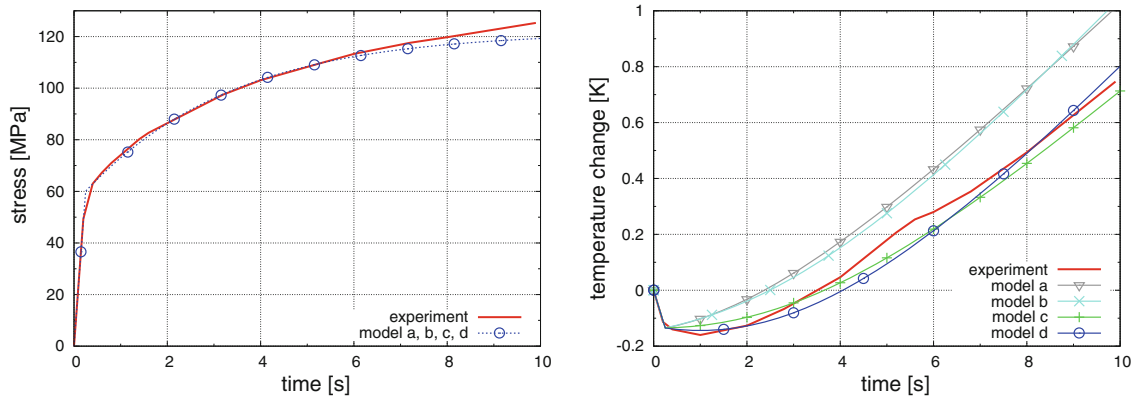


Fig. 6 Stress-time history (left) and temperature development (right) of experiment [13] and simulation

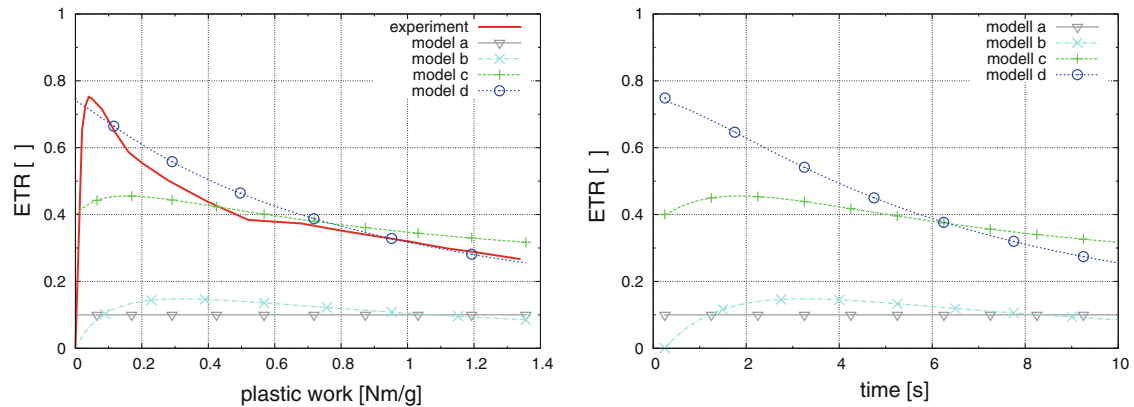


Fig. 7 Energy transformation ratio φ (ETR) of experiment [13] and simulation as a function of plastic work (left) and time (right)

The energy transformation ratios (ETR) of models (a) and (b) lie closely together, but both graphs are much too low compared to the experimental data—see Fig. 7, left picture. Hence, the energy storage capability of these models is too low. Accordingly, the simulated temperature curves are much higher than the experimental measurements—see Fig. 6, right picture. In the case of continuing plastic deformation, the ETR of model (b) would decrease further and soon tend to zero. On the other hand, the ETR for approach (a) remains constant.

Model (c) according to Helm [13] already shows a significantly improved agreement of the energy transformation ratio φ and the temperature development—see Fig. 6 (right) and 7 (left). However, initially the

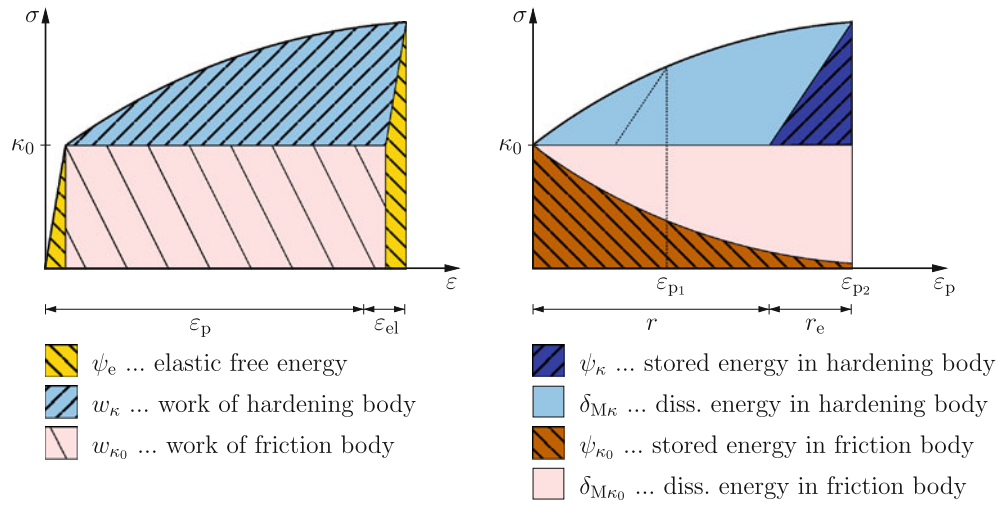


Fig. 8 Visualization of energy distribution with stored and dissipated parts

simulated ratio φ is still too low—but at the end of the calculation, it exceeds the curve determined from the experiment. In the case of continuously increasing equivalent plastic strain, the ETR, predicted by model (c), converges toward the value $\varphi^\infty = \beta_1 \frac{\kappa_0}{\kappa_0 + \kappa^\infty} \approx 0.2$. Thus, the energy storage is overestimated at further plastic loading and, hence, too low temperature values are predicted in the following course.

According to the experimental observations [3, 7, 13, 28, 29], the ETR of the enhanced energy storage model (d) follows a continuously falling trend and, thus, shows qualitatively and quantitatively good agreement with the test data—see Fig. 7 (left). Correspondingly, the differences between the simulated temperature course of approach (d) and the measured one are smallest (Fig. 6, right).

6 Studies of energy transformation behavior

6.1 Visualization of energy distribution

The energy partitioning under monotonic loading is presented for the special case of elastoplastic material behavior with pure isotropic hardening by means of the stress-strain diagrams in Fig. 8. In the left sketch, the stress is plotted versus the total strain. Hence, the area below the stress graph represents the entire mechanical work applied. At the left and the right hand side of this graph, the elastic fraction of the mechanical work is indicated. The area in between corresponds to the total plastic work, which is divided again into two fractions—namely the energy spent on the friction body (lower part) and the one applied to the hardening element (upper one).

The right diagram in Fig. 8 shows the stress plotted versus the plastic strain only. The area below the graph represents the total plastic work, decomposed again into the parts of the friction (below the stress κ_0) and the hardening body (above κ_0). In addition, stored and dissipated energy contributions are separated. The energy fraction $\psi_\kappa = \frac{1}{2} \kappa r_e = \frac{1}{2} E_\kappa r_e^2$, stored due to isotropic hardening, is identified as the triangular area marked in the diagram to the right analogously to the elastic work in the left one. The rate of the energy storage in the friction element, however, exhibits an exponentially decaying behavior as the plastic arclength augments—see (70) and (71). Thus, also its stored energy appears as a monotonically decreasing exponential function in the hardening diagram as visualized. Finally, the corresponding energy partitions are indicated in the right diagram at a previous state of plastic loading by means of the dashed lines.

6.2 Energy transformation in cyclic loading

For pure isotropic hardening, the increase in stored energy continues under cyclic loading until saturation of hardening is reached. In contrast to isotropic hardening, at the beginning of every load reversal, the entire energy, stored due to kinematic hardening, is released and dissipated as heat—but subsequently, the same

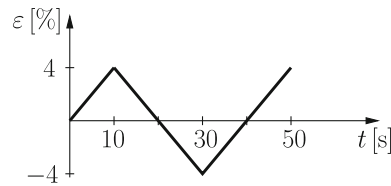


Fig. 9 Strain process of cyclic loading

Table 5 Hardening behavior and material parameters

Hardening type	Parameter	Label
Isotropic	$E_\kappa = 5,250.0 \text{ N/mm}^2$, $\kappa^\infty = 61.8 \text{ N/mm}^2$	iso
Isotropic / kinematic	$E_\kappa = E_\xi = 2,625.0 \text{ N/mm}^2$, $\kappa^\infty = \xi^\infty = 30.9 \text{ N/mm}^2$	iso/kin
Kinematic	$E_\xi = 5,250.0 \text{ N/mm}^2$, $\xi^\infty = 61.8 \text{ N/mm}^2$	kin

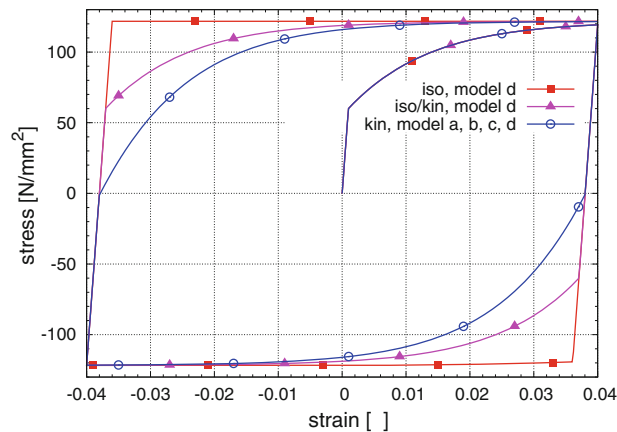


Fig. 10 Stress-strain diagram of cyclic loading

amount of energy is stored in every half-cycle of loading. In the case of ongoing cyclic loading, the total plastic work is continuously rising, and thus, the ETR of both, pure isotropic and kinematic hardening, tends to zero.

In the following study, the energy storage models as mentioned in Table 3 are subjected to the load path specified in Fig. 9. The new model (d) is applied with various hardening assumptions—see Table 5. However, only kinematic hardening is used for the approaches (a–c). In order to achieve a better quantification of the thermomechanical coupling effects, the following calculations are carried out under adiabatic conditions only. The parameters of the hardening models are summarized in Table 5, whereas the remaining ones are taken from Tables 3 and 4.

The isotropic hardening model converges comparatively fast toward its saturation limit for the set of parameters used—see Fig. 10. In the case of identical mechanical behavior with kinematic hardening, the four energy storage models (a–d) show the same stress response. As expected, the stress-strain diagram of the combined isotropic / kinematic hardening model is located between the adjacent stress curves.

The calculations with model (d) show the differences of the ETR between the isotropic and kinematic hardening approaches as well as the combined hardening model (Fig. 11, left). For the parameters chosen, the computed stress values are equal for all applied hardening types as the saturation limit is reached. Hence, at the end of every half-cycle of loading, nearly the same amount of energy is stored in all three hardening models, and thus, the ETR graphs calculated are nearly congruent to each other. Differences occur only directly after the points of load reversal, where energy is released initially in the case of kinematic hardening.

However, comparatively large differences exist between the simulated temperature courses (Fig. 11, right). One reason for this is: Directly after load reversal, the purely elastic domain of kinematic hardening is less than the one of isotropic hardening. Hence, thermoelastic heating or cooling—see (19) or (89)—is noticeably stronger for isotropic hardening (see Fig. 11, right). Another reason is that in the case of isotropic hardening, a higher stress level already exists at the beginning of the plastic domain after the points of load reversal. Thus, slightly more plastic work is spent afterwards than in the case of kinematic hardening. Accordingly, also the

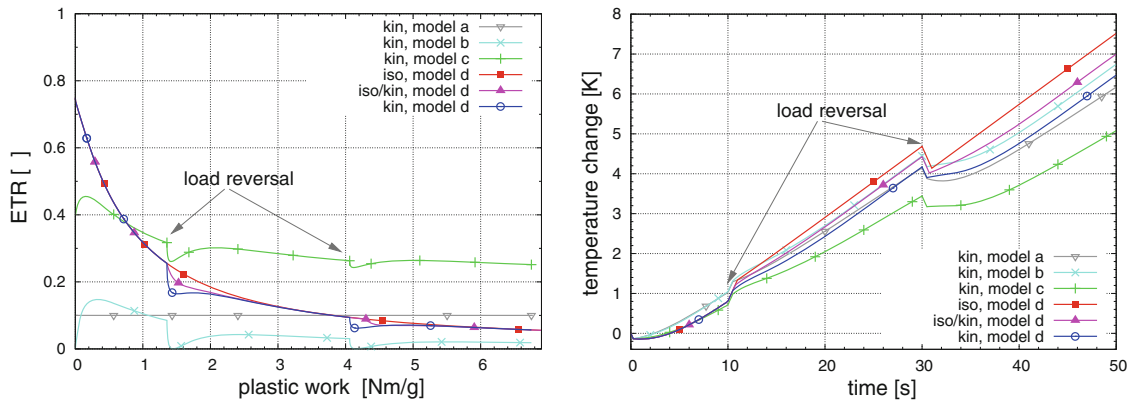


Fig. 11 Energy transformation ratio φ (ETR) and temperature development (adiabatic) in cyclic loading

Table 6 Parameter list for study of energy transformation in friction element

Set	#1	#2	#3	#4	#5	#6
β_1	0.0	0.2	0.4	0.75	0.75	0.75
β_2	0.0	0.0	0.0	10.0	60.0	400.0

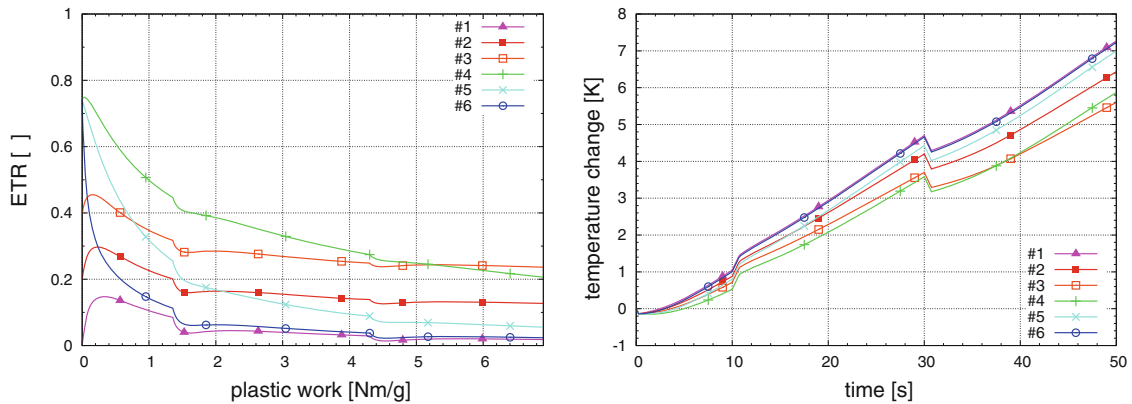


Fig. 12 Energy transformation ratio φ (ETR) and temperature development (adiabatic) of parameter study

dissipation of energy is slightly larger, which causes the somewhat higher temperature values in the analysis with isotropic hardening—see Fig. 11 (right).

In the calculations (a), (b) and (d), the total fraction of dissipated energy is higher or equal to 90 %, since the ETR at the end of the simulations is less or equal to 0.1 (see Fig. 11, left). The ETR of model (c) is considerably higher than in all other graphs, that is, a larger portion of plastic work is stored in the material—about 30 % in the calculation at hand. Thus, the resulting temperature is considerably lower than for the other models (Fig. 11, right). In contrast, model (b) does not store energy in the friction element and, hence, shows the lowest ETR diagram (Fig. 11, left). The associated course of temperature lies above the graph of model (d) with pure kinematic hardening (Fig. 11, right).

6.3 Parameter study of energy transformation in friction element

The study of approach (71), summarized in Table 6, is performed under cyclic loading with adiabatic conditions and combined isotropic / kinematic hardening. The remaining parameters are given in Table 4 and 5.

For the parameter sets #1 to #3, the associated graph of the energy transformation ratio moves upwards with a growing value β_1 , while the distance between these three curves remains nearly constant—see Fig. 12 (left). Thus, the differences between the related graphs of the temperature history continuously increase in the

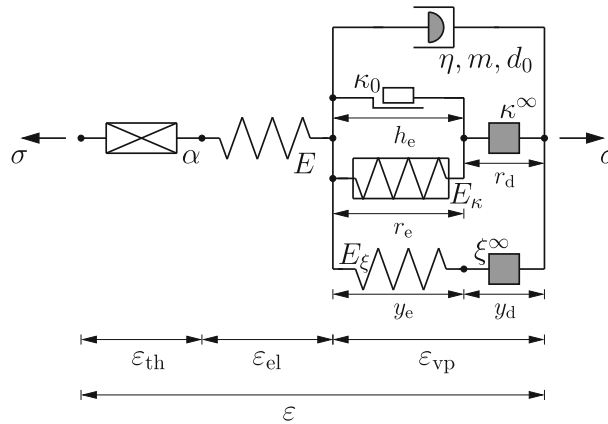


Fig. 13 Rheological model with modified energy storage in friction element

course of loading—see Fig. 12 (right). In all calculations for sets #4 to #6, the exponent β_2 is varied, while β_1 remains constant. Thus, the decay characteristic of the energy transformation ratio can be controlled: The smaller the parameter value β_2 is, the larger becomes the energy storage in the friction body—see Fig. 12 (left). For large values of β_2 , the graph of the ETR quickly converges toward curve #1, which neglects energy storage in the friction element.

7 Alternative models of energy storage

Approach 1

As demonstrated before, the approach in (71)—subsequently denoted as approach 1—is suitable to capture well the experimental energy storage behavior of metals, but requires the identification of both parameters β_1 and β_2 by means of the energy storage ratio obtained from experimental data or at least on the basis of a measured temperature history. However, if such data are not available, the usage of approach 1 is difficult. At the best, the user may choose appropriate parameter values due to his expert knowledge—or, again, it has to be resorted to the empirical estimate of the dissipation by means of the TAYLOR-QUINNEY coefficient—cf. (22).

For this reason, three alternative variants of approach 1 are proposed to control the energy storage in the friction element, which only need one or even not any additional material parameter. The modified constitutive model is implemented into the program MATLAB¹⁹ and validated by means of a comparison between the experimental data [13] and adiabatic calculations for a material point using the parameters as given in Tables 3 and 4 (line d).

Approach 2

The explanations concerning the kinematical requirements for the evolution equations of the internal strains h_d and r_d in Sect. 4.3 give reason to approach 2, where the evolution equation of h_d is chosen as equal to the one of r_d :

$$\dot{h}_d := \dot{r}_d = \frac{\kappa}{\kappa^\infty} \dot{\epsilon}_{vp}. \tag{90}$$

It corresponds to a rheological model with an assembly in parallel of a hardening and a friction body, arranged in series with only one shared dissipative strain element—see Fig. 13 and in comparison also Fig. 5. Hence, the energy storage behavior of the friction body is controlled in a natural way by the evolution of isotropic hardening, that is, energy storage occurs in the friction element only as long as the isotropic hardening variable enlarges. Thus, no additional material parameter is necessary in approach 2 to account for the storage of energy in the friction body.

¹⁹ MATLAB R2007a User Guides. Mathworks, 3 Apple Hill Drive, Natick, Massachusetts, USA.

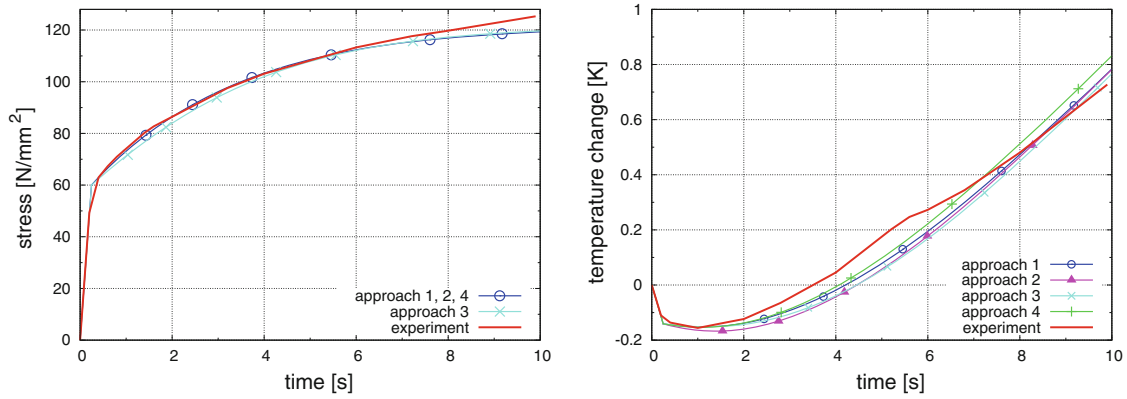


Fig. 14 Stress–strain diagram and temperature development (adiabatic) from alternative models of energy storage (exp. data of [13])

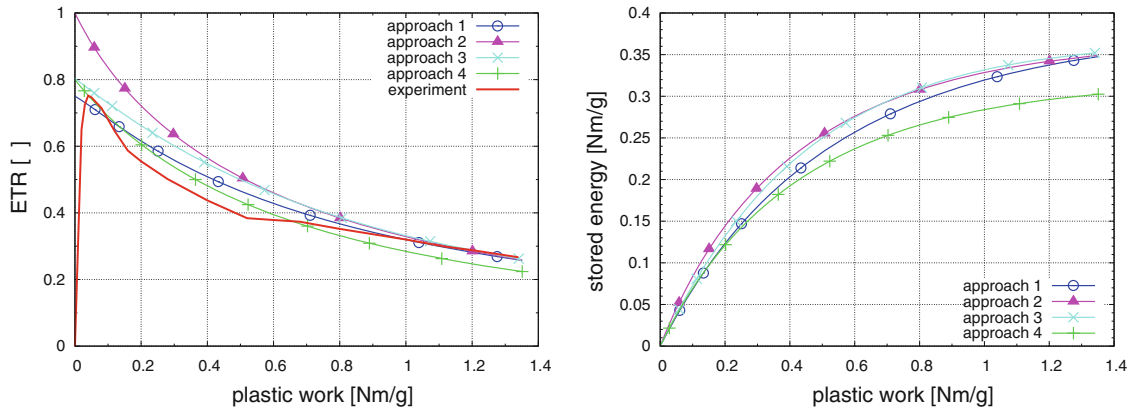


Fig. 15 Energy transformation ratio φ (ETR) and plastic stored energy from alternative models of energy storage (exp. data of [13])

At the beginning, the ETR of approach 2 shows a higher energy storage than model 1, adapted to the experimental data—see Fig. 15 (left). However, the differences between the associated curves 1 and 2 of the plastic stored energy are quite low—see Fig. 15 (right). In the course of plastic loading, the ETR curves 1 and 2 approach each other as well as the related graphs 1 and 2 of the plastic stored energy.

Approach 3

Since at the beginning, the energy storage ratio is too high in ansatz 2, the evolution equation of the internal strain r_d is modified in approach 3 as

$$\dot{h}_d = \dot{r}_d := \left(\frac{\kappa_0 + \kappa}{\kappa_0 + \kappa^\infty} \right)^n \dot{\varepsilon}_{vp}. \quad (91)$$

Obviously, approach 3 requires the determination of an additional material parameter n , which, however, is related to the constitutive approach with isotropic hardening and, thus, is identified by means of the experimental stress-strain history. Note, with (91) as well as (47) and (66), a slightly different evolution equation of the isotropic hardening variable κ results compared to the previous one in (73).

Ansatz 3 exhibits a similar decay characteristic of the ETR as model 2, if the isotropic hardening is increasing. However, the initial value $\dot{r}_d(\kappa = 0)$ results from the parameters κ_0, κ^∞ as well as n and is larger than zero in any case. Hence, in contrast to approach 2, the initial value of the energy transformation ratio of ansatz 3 is always less than one. With an exponent of $n = 2.3$, model 3 yields to a nearly identical stress-strain response as approaches 1 and 2—see Fig. 14 (left)—and the related course of the ETR and the plastic stored energy are very similar to ansatz 1 (Fig. 15).

Table 7 Comparison of energy storage models

Approach	Evolution equation \dot{h}_d	Resulting evolution equation \dot{h}_e
1	$\dot{h}_d := (1 - \beta_1 e^{-\beta_2 \bar{\epsilon}_{vp}}) \dot{\epsilon}_{vp}$	$\dot{h}_e = \beta_1 e^{-\beta_2 \bar{\epsilon}_{vp}} \dot{\epsilon}_{vp}$
2	$\dot{h}_d := \dot{r}_d = \frac{\kappa}{\kappa^\infty} \dot{\epsilon}_{vp}$	$\dot{h}_e = \left(1 - \frac{\kappa}{\kappa^\infty}\right) \dot{\epsilon}_{vp} = e^{-E_\kappa/\kappa^\infty \bar{\epsilon}_{vp}} \dot{\epsilon}_{vp}$
3	$\dot{h}_d := \dot{r}_d := \left(\frac{\kappa_0 + \kappa}{\kappa_0 + \kappa^\infty}\right)^{n_\kappa} \dot{\epsilon}_{vp}$	$\dot{h}_e = \left[1 - \left(\frac{\kappa_0 + \kappa}{\kappa_0 + \kappa^\infty}\right)^{n_\kappa}\right] \dot{\epsilon}_{vp}$
4	$\dot{h}_d := \left[1 - \beta \left(1 - \frac{\kappa}{\kappa^\infty}\right)\right] \dot{\epsilon}_{vp}$	$\dot{h}_e = \beta \dot{r}_c = \beta e^{-E_\kappa/\kappa^\infty \bar{\epsilon}_{vp}} \dot{\epsilon}_{vp}$

Approach 4

Combining version 1 and 2 of the evolution equations of \dot{h}_d , a further model variant (approach 4) is generated according to

$$\dot{h}_d := \left[1 - \beta \left(1 - \frac{\kappa}{\kappa^\infty}\right)\right] \dot{\epsilon}_{vp}. \quad (92)$$

Ansatz 4 corresponds to the rheological network represented in Fig. 5 with three dissipative strain elements. In contrast to approach 1, model 4 has merely one material parameter β , which must be identified by means of experimental data of the energy transformation behavior or by temperature measurements, respectively. However, the parameter β may also be estimated by an experienced user with expert knowledge, since β controls the initial value of the ETR course only, that is, it is always in the range between zero and one.

With a parameter value of $\beta = 0.8$, approach 4 yields to an ETR similar to the experiment—see Fig. 15. However, with increasing plastic deformation, the fraction of the plastic stored energy and, hence, the ETR are somewhat underestimated.

Comparison of alternative models of energy storage

The solution of the differential equation of isotropic hardening (73) for the initial condition $\kappa(0) = 0$ reads $\kappa = \kappa^\infty \left(1 - e^{-E_\kappa/\kappa^\infty \bar{\epsilon}_{vp}}\right)$, which may be used to transform the evolution equation \dot{h}_e of the approaches 2 and 4 as given in Table 7. Thus, both proposals 2 and 4 turn out for the values $\beta_2 = E_\kappa/\kappa^\infty$, $\beta_1 = 1$ or $\beta_1 = \beta$, respectively, as special cases of the energy storage approach 1.

8 Conclusions

An enhanced concept of rheological modeling is introduced, which enables a clearer representation of thermoviscoplastic material behavior with nonlinear isotropic and kinematic hardening, strain rate sensitivity as well as energy storage and dissipation during plastic deformation. In the framework of the balance equations of thermomechanics, a novel strategy is presented for deducing the constitutive relations of complex rheological models of thermoviscoplasticity by utilizing the network rules for serial and parallel assemblages as well as the defining equations of the basic rheological elements. By doing so, the yield function and the flow rule of the constitutive model are arising in a natural way.

In order to improve the prediction of energy transformation during plastic flow, four alternative approaches are proposed for modeling process-dependent energy storage in the friction element, allowing for a reliable description of the energy transformation behavior observed experimentally—partially even without the need for introducing any additional material parameters to account for the storage of energy, related to ideal plasticity.

Due to its well structured procedure and its high clarity, the concept presented for rheological modeling is also suitable especially for the purpose of education in science and research. Moreover, it may serve as a guidance for the development and characterization of further rheological assemblages with a more complex structure and new basic elements.

In a forthcoming publication, the proposed concept of enhanced rheological modeling is generalized to the three-dimensional application.

Acknowledgments The authors thankfully acknowledge the financial support of the German Research Foundation (DFG) through grant number Ma1186/5.

Table 8 Review of rheological bodies from literature

Material type	Rheological component	Abbreviation	Structural formula
Liquids (viscoelastic)	MAXWELL body	M	H — N
	LETHERSICH body	L ₁	N M
		L ₂	N — K
	TROUTON-RANKINE body	TR	N — PTH
	BURGERS body	BU	M — K
Solids (viscoelastic)	KELVIN body	K	H N
	POYNTING-THOMSON body	PTH	H M
	Thermal POYNTING-THOMSON body [19]	T-PTH	(H — T) (M — T)
Solids (elastoplastic)	PRANDTL body	P	H — ST.-V.
	Endochronic body [19]	EN	H — D
	KRAWIETZ body [19]	KRA	(EN ST.-V.) — H
Solids (elastoviscoplastic)	BINGHAM body	B	(N ST.-V.) — H
	SCHWEDOFF body	SCHW	(M ST.-V.) — H
	SCHOFIELD-SCOTT-BLAIR body	SCH SCB	B — K
	Modified SCHWEDOFF body [19]	MO-SCHW	(M P) — H
	Shape-Memory body ^a [19]	SH-ME	(H BL (N — ST.-V.)) — H
	LION body ^a [22]	LIO	EN H M
	Thermal LION body ^a [24]	T-LIO	T — LIO
Thermal KRAWIETZ body [23]	T-KRA	T — KRA	

^a Rheological body comprises nonlinear elastic spring

A Appendix

A.1 Remark on friction body

The friction element acts like two bodies sliding against each other in dry friction. To effect a nonzero strain ϵ in the ST.-VENANT's element, the magnitude of the applied external stress σ has to exceed the yield point κ_0 . The direction of strain evolution equals the direction of the applied stress:

$$\dot{\epsilon} \neq 0, \quad \text{sgn}(\dot{\epsilon}) = \text{sgn}(\sigma) \quad \text{for } |\sigma| = \kappa_0,$$

$$\dot{\epsilon} = 0 \quad \text{for } |\sigma| < \kappa_0.$$

However, as long as the yield point κ_0 is not reached, the friction element acts like a rigid body, that is, no strain emerges in this component. Formulating the stress as a function of the strain leads to the relation given in Table 1.

A.2 Review of various rheological bodies from literature

Further rheological bodies, given in [31] table 13 and 14, in [26,27] or proposed in [19,22,25,24,23], are summarized in Table 8 by means of their structural formula. As an alternative to the graphical representation of element assemblages, this formula specifies the basic elements and their compositions, which are included in the rheological network, and how they must be configured. The series connection of two elements E_1 and E_2 (Table 2 left) is represented by a horizontal line and results in the substitute element E_3 , whereas a vertical line indicates the parallel connection (Table 2 right) of the elements. In this review, the abbreviation “H” is used for HOOKE's body, whereas “N” and “ST.-V.” represent the NEWTON and the ST.-VENANT element. Moreover, the symbols “D” and “T” are used for the dissipative and the thermal strain bodies, specified in Sect. 3.3, and the abbreviation “BL” represents a blocking element, introduced by Krawietz [19], for the modeling of shape memory effects.

A.3 Free energy of thermal strain element

Since only thermal strains occur in the thermal strain element, the free energy, stored in this rheological component, and, therefore, the entropy are functions of the temperature only: $\psi = \psi(\theta)$ and $s = s(\theta)$. Hence, the free energy ψ can be calculated from the definition of the heat capacity at constant deformation c_{def} as in (18) and the potential equation of the entropy (7)—namely

$$c_{\text{def}}(\theta) = \theta \frac{\partial s(\theta)}{\partial \theta} = -\theta \frac{\partial^2 \psi(\theta)}{\partial \theta^2} \quad (93)$$

—after some rearrangements by means of integration with respect to temperature θ . In general, the heat capacity c_{def} is a function of the temperature: $c_{\text{def}} = c_{\text{def}}(\theta)$. Assuming a constant heat capacity $c_{\text{def}} = \text{const}$ and linearizing it at the temperature value $\theta = \theta_0$, the free energy of the thermal strain element can be calculated from (93) by double integration with respect to temperature θ :

$$\psi = -\frac{1}{2\theta_0} c_{\text{def}} \theta^2 + c_1 \theta + c_2. \quad (94)$$

The free constants c_1 and c_2 are determined from the initial conditions $\psi(\theta = \theta_0) = 0$ and $s(\theta = \theta_0) = 0$, which state that both the free energy (94) and the entropy (7) have to vanish for this rheological body at the reference temperature θ_0 . Thus, the free energy of the thermal strain element results as given in (39).

A.4 Review of mechanical dissipation

Two further formulations of the mechanical dissipation in (88) may be given from different points of view by means of (52) with (57) to (59) as well as (45, 47, 49) and (26)₂:

$$\delta_{\text{M}} = \frac{1}{\rho} (\sigma \dot{\epsilon}_{\text{vp}} - \sigma_{\kappa_0} \dot{h}_{\text{e}} - \sigma_{\kappa} \dot{r}_{\text{e}} - \sigma_{\xi} \dot{y}_{\text{e}}), \quad (95)$$

and by means of (69) with (44, 45, 47) and (49) as well as (63)₁, (65) and (26)₂:

$$\delta_{\text{M}} = \frac{1}{\rho} (\sigma_{\eta} \dot{\epsilon}_{\text{vp}} + \sigma_{\kappa_0} \dot{h}_{\text{d}} + \sigma_{\kappa} \dot{r}_{\text{d}} + \sigma_{\xi} \dot{y}_{\text{d}}). \quad (96)$$

In all variants of the mechanical dissipation (88, 95) and (96), each summand can be assigned directly to its corresponding basic component in the viscoplastic part of the rheological network in Fig. 5. In (95), the mechanical dissipation follows from the total viscoplastic stress power of the model less the power of stresses in the energy storing basic elements for friction and hardening as well as in the spring of kinematic hardening. On the other hand, the mechanical dissipation in (96) as well as in (88) is made up by the sum of the stress powers spent on the dissipative bodies, that is, in the dashpot and in the three dissipative strain elements.

A.5 Special cases of enhanced rheological model

Two special cases of the rheological network in Fig. 5 are discussed below.

Thermoplasticity

If the dashpot element is removed from the network in Fig. 5 or by driving the dashpot stress (44) to zero with $d(\dot{\epsilon}_{\text{p}}) \equiv 0$, rate-independent thermoviscoplasticity is recovered. The decomposed stress as in (43) and (77) with vanishing overstress $d(\dot{\epsilon}_{\text{p}}) = 0$ is separated into an equation of its absolute value and one for its algebraic sign, leading to

$$\text{sgn}(\sigma - \xi) = \text{sgn}(\dot{\epsilon}_{\text{p}}), \quad |\sigma - \xi| = (\kappa_0 + \kappa). \quad (97)$$

The first relation (97)₁ gives the direction of growth of the plastic strain rate $\dot{\varepsilon}_p = |\dot{\varepsilon}_p| \operatorname{sgn}(\dot{\varepsilon}_p)$. The second one in (97)₂ provides the yield function of thermoplasticity according to

$$f := |\sigma - \xi| - (\kappa_0 + \kappa) \equiv 0. \quad (98)$$

The argumentation to distinguish between the elastic and plastic domain is similar as before in the case of thermoviscoelasticity—cf. Sect. 4.4. Hence, no elastoplastic flow may occur for $f < 0$ and (97) holds only for states of $f \equiv 0$. In contrast to viscoplasticity, values of $f > 0$ are impossible for rate-independent plasticity, and furthermore, no constitutive equation exists for a closed form calculation—cf. (84)—of the plastic multiplier $\lambda := |\dot{\varepsilon}_p|$, which may be determined from the yield condition $f \equiv 0$ in (98) or from the related consistency condition of plasticity

$$\dot{f} = \frac{\partial f}{\partial \sigma} \dot{\sigma} + \frac{\partial f}{\partial \xi} \dot{\xi} + \frac{\partial f}{\partial \kappa} \dot{\kappa} = 0. \quad (99)$$

Due to the identity $f \equiv 0$, the first term of the mechanical dissipation in (88) or (96) vanishes in the case of the rate-independent plasticity²⁰.

Thermoviscoelasticity

For the special case of $\kappa_0 = 0$ and $\kappa \equiv 0$, the yield function (81) is satisfied trivially and, hence, the material model behaves purely thermoviscoelastic. Thereby, both branches of the rheological model in Fig. 5 for the friction and hardening body remain stress free, and thus, may be omitted. By setting the internal strain variable y_d identical to zero in the lowest dissipative strain element (Fig. 5), the rheological network turns into a thermoviscoelastic model of the KELVIN type and the mechanical dissipation reduces to the first term of (96) or the first summand of the product in (88).

A.6 Comparison of alternative approaches of thermoelastic free energy

Instead of the strain decomposition (2), it is common in thermoviscoplastic modeling to divide the total strain into a (thermo)-elastic and an inelastic part according to²¹

$$\varepsilon = \varepsilon_{te} + \varepsilon_i \quad (100)$$

only, where the strain part ε_{te} contains both elastic and thermal contributions. Hence, the thermoelastic part of the related free energy is usually assumed according to the classical approach of thermoelasticity as a function of the thermoelastic strain ε_{te} and the temperature θ :

$$\psi(\varepsilon_{te}, \theta) = \frac{1}{\rho} \left[\frac{1}{2} E \varepsilon_{te}^2 - E \alpha (\theta - \theta_0) \varepsilon_{te} - \frac{1}{2\theta_0} \rho c_{\text{def}} (\theta - \theta_0)^2 \right] \quad (101)$$

—see also [10, 11, 13–16, 21, 26, 43]²². Since both alternative approaches of the thermoelastic free energy (51)₂ and (101) do not originate the same constitutive model, the arising differences are investigated in this section for the interested reader²³.

According to the potential relations of classical thermoelasticity²⁴, the stress and the entropy are calculated from the free energy term in (101) as

$$\sigma = \rho \frac{\partial \psi}{\partial \varepsilon_{te}} = E [\varepsilon_{te} - \alpha (\theta - \theta_0)], \quad s = \rho \frac{\partial \psi}{\partial \varepsilon_{te}} = \frac{1}{\rho} E \alpha \varepsilon_{te} + \frac{1}{\theta_0} c_{\text{def}} (\theta - \theta_0) \quad (102)$$

²⁰ It is proven analytically in [10, 16, 38] that the material equations of viscoplasticity with the flow rule according to (85) (for the special case $m = 1$) turn into the rate-independent equations of plasticity for the vanishing parameter $\eta \rightarrow 0$ or in a quasi-static process.

²¹ In the literature, the first summand of (100) is usually denoted as ε_{el} .

²² This approach of the free energy may be justified as follows: The first two terms result from the integration of the stress relation $\sigma = E [\varepsilon - \alpha (\theta - \theta_0)]$ with respect to the strain ε , whereas the last summand is obtained by integrating the definition of the heat capacity as shown in Appendix A.3.

²³ The following considerations are given for the special case of thermoelastic material behavior, since the arising differences only affect this part of the constitutive model.

²⁴ In contrast to the potential equation for the entropy (7), the well-known relation (102)₃ contains only one single term. The additional summand in (7) results from the separated thermal strain part ε_{th} in (2) and its associated evolution equation (3) for the thermal strain rate—see also [23].

and the equation of heat conduction becomes—see e.g., [10]:

$$c_{\text{def}} \dot{\theta} = -\frac{1}{\rho} E \alpha \theta \dot{\varepsilon}_{\text{te}} + \frac{1}{\rho} k \operatorname{div}(g) + b. \quad (103)$$

Only in order to better compare the mathematical structure of both representations of the free energy (51)₂ and (101), the thermoelastic strain ε_{te} at hand may be decomposed formally also into a purely elastic and a thermal part

$$\varepsilon_{\text{te}} = \varepsilon_{\text{el}} + \varepsilon_{\text{th}}, \quad (104)$$

although this partition might not be meaningful in physical sense or intended in classical thermoelasticity. In accordance with the stress relation (102)₂, the latter one is computed as given in (38). The split (104) allows to transform the free energy of (101) into the expression

$$\psi(\varepsilon_{\text{el}}, \theta) = \frac{1}{\rho} \left[\frac{1}{2} E \varepsilon_{\text{el}}^2 - \frac{1}{2} E \varepsilon_{\text{th}}^2 - \frac{1}{2\theta_0} \rho c_{\text{def}} (\theta - \theta_0)^2 \right]. \quad (105)$$

Compared to the approach for the free energy in (51)₂, the summand $-\frac{1}{2} E \varepsilon_{\text{th}}^2$ appears as an additional negative energy contribution in (105) as a consequence of the coupling term $-E\alpha(\theta - \theta_0)\varepsilon_{\text{te}}$ in the free energy expression in (101) and is discussed by means of the subsequent thought experiment.

A thermoelastic rod with free ends is considered under thermomechanical loading:

In the first step, the rod is heated up to the temperature level θ_1 causing inevitably the thermal strain $\varepsilon_{\text{th}} = \alpha(\theta_1 - \theta_0)$. However, due to the boundary conditions given, no stress is induced in the rod during heating, that is, the elastic strain vanishes $\varepsilon_{\text{el}} = 0$ and the total strain is equal to the thermal one: $\varepsilon_{\text{te}} = \varepsilon_{\text{th}}$. According to the free energy assumption (51)₂, only the heat energy $\psi_{\text{th}} = -c_{\text{def}}(\theta_1 - \theta_0)^2/(2\theta_0)$ is rationally stored in the rheological model due to the thermal loading process specified above. However, compared to the free energy term (51)₂, an unexpected additional energy contribution $\tilde{\psi}_{\text{th}} = -E\varepsilon_{\text{th}}^2/(2\rho)$ obviously arises in the expression of the free energy (105).

In a second process step, the hot rod is compressed isothermally by driving the total strain to zero: $\varepsilon_{\text{te}} = 0$. Hence, the equality $\varepsilon_{\text{el}} = -\varepsilon_{\text{th}}$ results for the elastic and the thermal part of the strain. In the free energy assumption of the rheological model (51)₂, the compression applied causes an elastic energy storage of $\psi_{\text{el}} = E\varepsilon_{\text{el}}^2/(2\rho)$ due to the elastic strains besides the existing thermal contribution ψ_{th} , that is, $\psi = \psi_{\text{el}} + \psi_{\text{th}}$ results. However, in the free energy term (105), the first two terms cancel each other for the thermomechanical loading given. Hence, only the energy $\psi = \psi_{\text{th}}$ is stored in this case, although the stress $\sigma = -E\alpha(\theta_1 - \theta_0)$ certainly governs the elastic rod deformation.

In view of these contradicting conclusions, only the free energy of the rheological model according to (51)₂ offers physically reasonable results for both the thermal and the mechanical loading step.

The evaluation of (102) and (103) by means of the assumption (104) provides the stress

$$\sigma = E\varepsilon_{\text{el}}, \quad (106)$$

which is identical to the one of the rheological model in (86)₁ from Sect. 4.5. However, the entropy relation

$$s = \frac{1}{\rho} E \alpha (\varepsilon_{\text{el}} + \varepsilon_{\text{th}}) + \frac{1}{\theta_0} c_{\text{def}} (\theta - \theta_0), \quad (107)$$

emerging from (102)₄, as well as the equation of heat conduction

$$c_{\text{def}} \dot{\theta} = -\underbrace{\frac{1}{\rho} E \alpha \theta (\dot{\varepsilon}_{\text{el}} + \dot{\varepsilon}_{\text{th}})}_{-p_e} + \frac{1}{\rho} k \operatorname{div}(g) + b \quad (108)$$

following from (103), deviate from the corresponding expressions in Sect. 4.5: The first term on the right-hand side of (107) and (108) contains the sum of elastic and thermal strain or their rates. In contrast, only the elastic strain or its rate appears in the corresponding term of the material equations (86)₂ and (89) from the rheological model.

The structure of the thermoelastic coupling term

$$p_e = -\frac{1}{\rho} E \alpha \theta (\dot{\epsilon}_{el} + \dot{\epsilon}_{th}) = -\frac{1}{\rho} E \alpha \theta (\dot{\epsilon}_{el} + \alpha \dot{\theta}) \quad (109)$$

in the equation of heat conduction (108) leads obviously to the following consequence: The elastic strain rate $\dot{\epsilon}_{el}$, which is a purely mechanical quantity, affects a positive or negative heat contribution to p_e . Moreover, if, for example, the body is heated externally, that is, $\dot{\theta} > 0$ holds, then the thermal strain rate $\dot{\epsilon}_{th}$, driven by temperature change according to (3), in turn causes negative heat production and, surprisingly, reduces the temperature rise as a consequence of the mathematical structure of the thermoelastic coupling term p_e in (109). On the other hand, the structure of the thermoelastic coupling term appears as expected and more reasonable in the equation of heat conduction (89) of the constitutive model in Sect. 4.5.

Note, if the free energy (101) and the thermoelastic coupling term in (103) are considered without the rearrangements by means of the formal strain decomposition in (104), identical conclusions may be drawn as documented above.

Therefore, the decomposition of the strain according to (2) and the associated representation of the thermoelastic free energy in (51)₂ are not only suitable for the concept of rheological modeling as proposed, but also lead to more general material equations and, thus, appear advantageously in comparison to classical approach of thermoelasticity in (101).

References

1. Altenbach, J., Altenbach, H.: Einführung in die Kontinuumsmechanik. Teubner, Stuttgart (1994)
2. Armstrong, P.J., Frederick, C.O.: A Mathematical Representation of the Multiaxial Bauschinger Effect. General Electricity Generating Board, Report No. RD/B/N731 (1966)
3. Bever, M.B., Holt, D.L., Titchener, A.L.: The Stored Energy of Cold Work. Pergamon Press, Oxford (1973)
4. Bröcker, C., Matzenmiller, A.: Thermoviscoplasticity deduced from enhanced rheological models. PAMM **12**, 1–2 (2012)
5. Chaboche, J.L.: Cyclic viscoplastic constitutive equations, part I: a thermodynamically consistent formulation. J. Appl. Mech. **60**, 813–821 (1993)
6. Chaboche, J.L.: Cyclic viscoplastic constitutive equations, part II: stored energy—comparison between models and experiments. J. Appl. Mech. **60**, 822–828 (1993)
7. Chrysochoos, A., Maisonneuve, O., Martin, G., Caumon, H., Chezeaux, J.C.: Plastic and dissipated work and stored energy. Nucl. Eng. Des. **114**, 323–333 (1989)
8. Findley, W.N., Lai, J.S., Onaran, K.: Creep and Relaxation of Nonlinear Viscoelastic Materials. Dover Publication, New York (1989)
9. Giesekus, H.: Phänomenologische Rheologie. Springer, Berlin (1994)
10. Haupt, P.: Continuum Mechanics and Theory of Materials. Springer, Berlin (2002)
11. Haupt, P.: Theory of materials: summarizing remarks. In: Bruhns, O.T., Meyers, A. (eds.) Proceedings of 9th International Symposium on Plasticity and Impact Mechanics. The University Press Bochum (2007)
12. Haupt, P., Helm, D., Tsakmakis, C.: Stored energy and dissipation in thermoviscoplasticity. ZAMM **77**, S119–S120 (1997)
13. Helm, D.: Experimentelle Untersuchung und phänomenologische Modellierung thermomechanischer Kopplungseffekte in der Metallplastizität. In: Hartmann, S., Tsakmakis, C. (eds.) Aspekte der Kontinuumsmechanik und Materialtheorie. Report 1/1998 of the Institute of Mechanics, University of Kassel, Moenchebergstr. 7, Kassel (1998)
14. Helm, D.: Stress computation in finite thermoviscoplasticity. Int. J. Plast. **22**, 1699–1727 (2006)
15. Jansohn, W.: Formulierung und Integration von Stoffgesetzen zur Beschreibung großer Deformationen in der Thermoplastizität und -viskoplastizität. Doctoral Thesis, Scientific reports FZKA-6002, Institute for Materials Research, Research Center Karlsruhe, Kaiserstr. 12, Karlsruhe (1997)
16. Kamlah, M.: Zur Modellierung des Verfestigungsverhaltens von Materialien mit statischer Hysterese im Rahmen der phänomenologischen Thermomechanik. Doctoral Thesis, Report 3/1994 of the Institute of Mechanics, University of Kassel, Moenchebergstr. 7, Kassel (1994)
17. Kamlah, M., Haupt, P.: On the macroscopic description of stored energy and self heating during plastic deformation. Int. J. Plast. **13**, 893–911 (1998)
18. Kletschkowski, T., Schomburg, U., Bertram, A.: Viskoplastische Materialmodellierung am Beispiel des Dichtungswerkstoffes Polytetrafluorethylen. Technische Mechanik **21**, 227–241 (2001)
19. Krawietz, A.: Materialtheorie. Springer, Berlin (1986)
20. Krempl, E., McMahon, J.J., Yao, D.: Viscoplasticity based on overstress with a differential growth law for the equilibrium stress. Mech. Mater. **5**, 35–48 (1986)
21. Lemaitre, J., Chaboche, J.L.: Mechanics of Solid Materials. Cambridge University Press, Cambridge (1990)
22. Lion, A.: A physically based method to represent the thermo-mechanical behaviour of elastomers. Acta Mech. **123**, 1–25 (1997)
23. Lion, A.: Constitutive modelling in finite thermoviscoplasticity: a physical approach based on nonlinear rheological models. Int. J. Plast. **16**, 469–494 (2000a)
24. Lion, A.: Thermomechanik von Elastomeren: Experimente und Materialtheorie. Habilitation Thesis, Report 1/2000 of the Institute of Mechanics, University of Kassel, Moenchebergstr. 7, Kassel. <http://nbn-resolving.de/urn:nbn:de:hebis:34-2007092619247> (2000b)

25. Lion, A., Sedlan, K.: Finite Thermoviskoplastizität: Eine Methode zur Formulierung thermodynamisch konsistenter Stoffgleichungen. In: Hartmann, S., Tsakmakis, C. (eds.) *Aspekte der Kontinuumsmechanik und Materialtheorie*. Report 1/1998 of the Institute of Mechanics, University of Kassel, Moenchebergstr. 7, Kassel (1998)
26. Maugin, G.A.: *The Thermomechanics of Plasticity and Fracture*. Cambridge University Press, Cambridge (1992)
27. Meinhard, H.: *Rheologische Untersuchungen zu Härteeindruckexperimenten im Nanometerbereich*. Doctoral Thesis, Institute of Physics, Martin-Luther-University Halle-Wittenberg, Betty-Heimann-Str. 7, Halle. <http://nbn-resolving.de/urn/resolver.pl?urn=nbn:de:gbv:3-000000239> (1999)
28. Oliferuk, W., Gadaj, S.P., Grabski, M.W.: Energy storage during the tensile deformation of armco iron and austenitic steel. *Mater. Sci. Eng.* **70**, 131–141 (1985)
29. Oliferuk, W., Maj, M., Raniecki, B.: Experimental analysis of energy storage rate components during tensile deformation of polycrystals. *Mater. Sci. Eng. A* **374**, 77–81 (2004)
30. Perżyna, P.: The constitutive equations for rate sensitive plastic materials. *Q. Appl. Math.* **20**, 321–332 (1963)
31. Reiner, M.: *Rheologie in elementarer Darstellung*. Carl Hanser Verlag, München (1969)
32. Rieger, S.: *Temperaturabhängige Beschreibung visko-elasto-plastischer Deformationen kurzglasfaserverstärkter Thermoplaste. Modellbildung, Numerik und Experimente*. Doctoral Thesis, Institute of Applied Mechanics (Civil Engineering), University Stuttgart, Pfaffenwaldring 7, Stuttgart. <http://nbn-resolving.de/urn:nbn:de:bsz:93-opus-19462> (2004)
33. Shutov, A., Panhans, S., Kreißig, R.: A phenomenological model of finite strain viscoplasticity with distortional hardening. *J. Appl. Math. Mech.* **91**(8), 653–680 (2011)
34. Shutov, A.V., Ihlemann, J.: On the simulation of plastic forming under consideration of thermal effects. *Materialwissenschaft und Werkstofftechnik* **42**, 632–638 (2011)
35. Simo, J., Miehe, C.: Associative coupled thermoplasticity at finite strains: formulation, numerical analysis and implementation. *Comput. Methods Appl. Mech. Eng.* **98**(1), 41–104 (1992)
36. Simo, J.C., Hughes, T.J.R.: *Computational Inelasticity*. Springer, New York (1998)
37. Taylor, G.I., Quinney, H.: The latent energy remaining in a metal after cold working. *Proc. R. Soc. Lond. Ser. A Math. Phys. Sci.* **143**, 307–326 (1934)
38. Tsakmakis, C.: *Methoden zur Darstellung inelastischen Materialverhaltens bei kleinen Deformationen*. Habilitation Thesis, Report 5/1994 of the Institute of Mechanics, University of Kassel, Moenchebergstr. 7, Kassel. <http://nbn-resolving.de/urn:nbn:de:hebis:34-2007102419481> (1994)
39. Tschoegl, N.W.: *The Phenomenological Theory of Linear Viscoelastic Behavior*. Springer, Berlin (1989)
40. Valanis, K.C.: A theory of viscoplasticity without a yield surface: part I, general theory. *Arch. Mech.* **23**, 517–533 (1971)
41. Visintin, A.: Mathematical models of hysteresis. In: Bertotti, G., Mayergoyz, I.D. (eds.) *The Science of Hysteresis*, vol. 1, Elsevier, Amsterdam (2006)
42. Wriggers, P.: *Nichtlineare Finite-Element-Methoden*. Springer, Berlin (2001)
43. Ziegler, H.: *An Introduction to Thermomechanics*. North-Holland, Amsterdam (1977)